



## Review

Amyloid  $\beta$  interaction with model cell membranes – What are the toxicity-defining properties of amyloid  $\beta$ ?Dusan Mrdenovic<sup>a,b</sup>, Izabela S. Pieta<sup>a</sup>, Robert Nowakowski<sup>a</sup>, Włodzimierz Kutner<sup>a,c</sup>, Jacek Lipkowski<sup>b</sup>, Piotr Pieta<sup>a,\*</sup><sup>a</sup> Institute of Physical Chemistry, Polish Academy of Sciences, Kasprzaka 44/52, 01-224 Warsaw, Poland<sup>b</sup> Department of Chemistry, University of Guelph, 50 Stone Road East, Guelph, Ontario N1G 2W1, Canada<sup>c</sup> Faculty of Mathematics and Natural Sciences, School of Sciences, Cardinal Stefan Wyszyński University in Warsaw, Wóycickiego 1/3, 01-815 Warsaw, Poland

## ARTICLE INFO

## Keywords:

Amyloids  
Aggregation  
Lipids  
Membranes  
Permeation

## ABSTRACT

Disruption of the neuronal membrane by toxic amyloid  $\beta$  oligomers is hypothesized to be the major event associated with Alzheimer's disease's neurotoxicity. Misfolding of amyloid  $\beta$  is followed by aggregation via different pathways in which structurally different amyloid  $\beta$  oligomers can be formed. The respective toxic actions of these structurally diverse oligomers can vary significantly. Linking a particular toxic action to a structurally unique kind of amyloid  $\beta$  oligomers and resolving their toxicity-determining feature remains challenging because of their transient stability and heterogeneity. Moreover, the lipids that make up the membrane affect amyloid  $\beta$  oligomers' behavior, thus adding to the problem's complexity. The present review compares and analyzes the latest results to improve understanding of amyloid  $\beta$  oligomers' interaction with lipid bilayers.

## 1. Introduction

Alzheimer's disease (AD) was first diagnosed about a century ago [1]. Since then, many efforts have been put into understanding the origin and development of this lethal disease. Significant progress has been made in comprehending the causes and pathophysiology of AD. However, many questions are still left unanswered, and AD remains incurable.

The amyloid cascade hypothesis states that the amyloid  $\beta$  (A $\beta$ ) protein plays a central role in AD development [2]. According to this hypothesis, the A $\beta$  over-production, aggregation, and accumulation in the human brain trigger a cascade of molecular and cellular events leading to a progressive synaptic and neuritic injury, disturbance of ionic homeostasis, oxidative damage of cells that result in neuronal death, and consequently, dementia [3].

A $\beta$  is a 39–42 amino acid-long peptide produced from proteolytic cleavage of transmembrane amyloid precursor protein (APP) by  $\beta$ - and  $\gamma$ -secretase [4,5]. In its native form, A $\beta$  exhibits neuroprotective abilities and stimulates brain development [6]. However, A $\beta$  misfolding and overproduction, as well as imbalance in the A $\beta_{40}$ -to-A $\beta_{42}$  ratio, lead to the development of pathological conditions. Moreover, the native state of any protein, even though thermodynamically favorable, is not

necessarily stable. A protein or polypeptide consisting of  $\sim 100$  amino acids can adopt as many as  $10^{49}$  conformations [7]. The cellular environment in the human body contains a quality control system (QCS). This system consists of molecular chaperones and the ubiquitin-proteasome system [8,9]. The role of this system is to help proteins adopt their native folding and degrade misfolded proteins. Malfunctioning of QCS and the intrinsic nature of proteins to adopt many non-native conformations are the reasons why protein folding is error-prone, thus resulting in protein misfolding [10].

The A $\beta$  misfolding and overproduction lead to its aggregation. The A $\beta$  aggregation mechanism (Fig. 1) is under debate, and many different aggregation pathways have been proposed [11–19]. The nucleation-dependent aggregation of A $\beta$  monomers (A $\beta$ Ms), known as “on-pathway” aggregation, leads to the formation of various forms of ( $\beta$ -sheet)-rich aggregates such as spherical A $\beta$  oligomers (A $\beta$ Os), elongated protofibrils and mature A $\beta$  fibrils (A $\beta$ Fs) with the cross- $\beta$  structure where individual strands are perpendicular to the fibril axis [11–13]. Moreover, A $\beta$ Ms can aggregate “off-pathway,” thus forming unstructured, amorphous aggregates [14,15]. These “off-pathway” aggregates can dissociate into lower-molecular-weight aggregates that can aggregate “on-pathway.” Furthermore, “on-pathway” aggregates can dissociate (aggregate fragmentation) [16,20]. As a result of these complex

\* Corresponding author.

E-mail address: [ppieta@ichf.edu.pl](mailto:ppieta@ichf.edu.pl) (P. Pieta).<https://doi.org/10.1016/j.ijbiomac.2022.01.117>

Received 24 November 2021; Received in revised form 10 January 2022; Accepted 18 January 2022

Available online 21 January 2022

0141-8130/© 2022 The Authors. Published by Elsevier B.V. This is an open access article under the CC BY license (<http://creativecommons.org/licenses/by/4.0/>).

processes, many different A $\beta$  aggregates may coexist.

While most studies consider A $\beta$ M and A $\beta$ Fs as non-toxic [25–27], the acceptance of A $\beta$ O as the most toxic and pathogenic form of A $\beta$  leads to the so-called Amyloid  $\beta$  Oligomer Hypothesis [28]. A $\beta$ O can cause learning and cognition deficiency [29,30], deterioration of synapses [31,32], triggering of cell death via leakage of lysosomal enzymes [33], inhibition of mitochondrial activity [34], the increase of production of reactive oxygen species [35], or neuroinflammation [36,37]. Moreover, A $\beta$ O can permeate cell membranes according to different mechanisms, including pore/ion channel formation [38–40] and lipid extraction (Fig. 2) [41–46]. Apparently, A $\beta$ O can exert a whole range of different toxic effects. Still, it is not clear which is their preferential pathological activity.

Difficulties in purification and handling this sensitive peptide lead to many experimental problems and, hence, the irreproducibility of results of different research groups. Therefore, A $\beta$  is named “the peptide from hell” [47,48]. Various research groups developed different A $\beta$  preparation procedures [49–51] to resolve these issues. These procedures result in different aggregation kinetics, aggregation pathways, and type of aggregates produced, thus challenging comparison of published results. It is essential to determine A $\beta$ O structural properties to distinguish between their different types and their respective toxic actions. Classification of A $\beta$ O by their uniqueness in structure and toxicity would explain which protein feature is responsible for a specific toxic effect exerted by a given kind of A $\beta$ O. Moreover, this information would allow one to design appropriate therapeutic approaches specifically targeting each A $\beta$ O type. Unfortunately, the polymorphic nature, heterogeneity, and transient stability of A $\beta$ O make the determination of their structural properties challenging [52]. Nevertheless, certain progress has been made in revealing the structural features of A $\beta$ O that define their toxicity. Some studies imply that small, low-molecular-weight (LMW) [26,27,43,53,54] and highly hydrophobic [55–58] A $\beta$ O are the most toxic. LMW A $\beta$ O range from dimers to pentamers, while a molecular weight of high-molecular-weight (HMW) A $\beta$ O is higher than that of pentamers [27]. However, this A $\beta$ O classification is based on individual measurements, thus varies from study to study [59,60].

On the contrary, other studies suggest that large A $\beta$ O are more toxic than small oligomers [58,61]. Some studies indicate a lack of difference in toxicity between small and large A $\beta$ O, but their respective toxic actions are different. That is, small A $\beta$ O permeate lipid membranes, while large A $\beta$ O induce cell inflammation [53,54]. Interestingly, size-independent A $\beta$ O toxicity, influenced by distinct A $\beta$ O conformations, was also observed. Both ( $\beta$ -sheet)-rich A $\beta$ O [62–64] and unstructured A $\beta$ O (abundant in a random coil secondary structure) [57,65,66] are toxic.

Since there are discrepancies between published results, a comparison and a critical analysis of the latest findings are needed. An in-depth consideration of the contradictory results may explain these

discrepancies and reveal the unanswered questions that could be addressed in future research. Therefore, the goal of the present review is to pinpoint (i) structural properties of A $\beta$ O crucial for the particular mechanism of toxicity or aggregation on a lipid membrane, (ii) changes in the membrane properties that might inhibit or facilitate those actions, and (iii) unanswered questions that might stimulate new research giving a more in-depth insight into the A $\beta$ -lipid interaction.

## 2. Ion channels in bilayer lipid membranes

Ion channels are donut-shaped pores with outer and inner diameters of  $\sim 10$  and  $1\text{--}2$  nm, respectively, that protrude  $\sim 0.5$  nm above the membrane surface (Fig. 3a) [39,40,67–71]. A $\beta_{40}$  can form Ca $^{2+}$ -permeable channels in 1-palmitoyl-2-oleoyl-*sn*-glycero-3-phosphoethanolamine (POPE) or POPE/1-palmitoyl-2-oleoyl-*sn*-glycero-3-phosphoserine (POPS) lipid bilayers. From this observation, it follows that disruption of Ca $^{2+}$  cell homeostasis leads to neuronal death characteristic of AD [38,72]. Small A $\beta_{40}$  oligomers, ranging from trimers to hexamers, form ion channels in the 1,2-dioleoyl-*sn*-glycero-3-phosphocholine (DOPC) membrane [39,40]. The formation of multiple electrical conductance states agrees with the presence of ion channels formed by oligomers of different molecular weights (Fig. 3b) [39,40,72–75]. In contrast, A $\beta_{40}$ O were incapable of ion channels forming in the membrane excised from HEK293 cells [76]. This behavior was also observed for A $\beta_{40}$ M and fibrils (A $\beta_{40}$ F), as well as A $\beta_{42}$ M and A $\beta_{42}$ F, while only A $\beta_{42}$ O with 5–20 nm in diameter were capable of forming ion channels. Moreover, A $\beta_{40}$ M, unlike A $\beta_{42}$ M and A $\beta_{42}$ O, do not porate the membrane. Instead, they fibrillate on the surface of the dodecylphosphocholine (DPC), octyl glucoside (OG), and 1,2-dihexanoyl-*sn*-glycero-3-phosphocholine (DHPC) membranes [69]. Interestingly, both A $\beta_{42}$ M and A $\beta_{42}$ O porate lipid bilayers and induce different types of ionic currents. A $\beta_{42}$ M induce fast, transient, and heterogeneous, so-called “spiky” ionic currents that indicate the formation of a heterogeneous population of pores. Monomers cannot be heterogeneous. This monomer property rules out the possibility that A $\beta_{42}$ M themselves form ion channels with heterogeneous ionic currents in the lipid membrane. Most likely, A $\beta_{42}$ M aggregate into A $\beta_{42}$ O of different sizes and molecular weights that produce variable-size ion channels of diverse electrical activity.

On the other hand, the addition of pre-formed A $\beta_{42}$ O results in the formation of three distinct types of ionic currents that are different from those in the presence of A $\beta_{42}$ M. The pre-formed A $\beta_{42}$ O are rich in the  $\beta$ -sheet secondary structure and are barrel-like arranged in lipid bilayers, thus they are referred to as “ $\beta$ -barrel pore-forming A $\beta_{42}$  oligomers”. In the presence of fresh A $\beta_{42}$ M and pre-formed A $\beta_{42}$ O, different types of ionic currents were recorded for each bilayer system [69]. These different ionic currents indicate that A $\beta_{42}$ O and A $\beta_{42}$ O pre-formed from A $\beta_{42}$ M, which aggregated on the membrane, generated

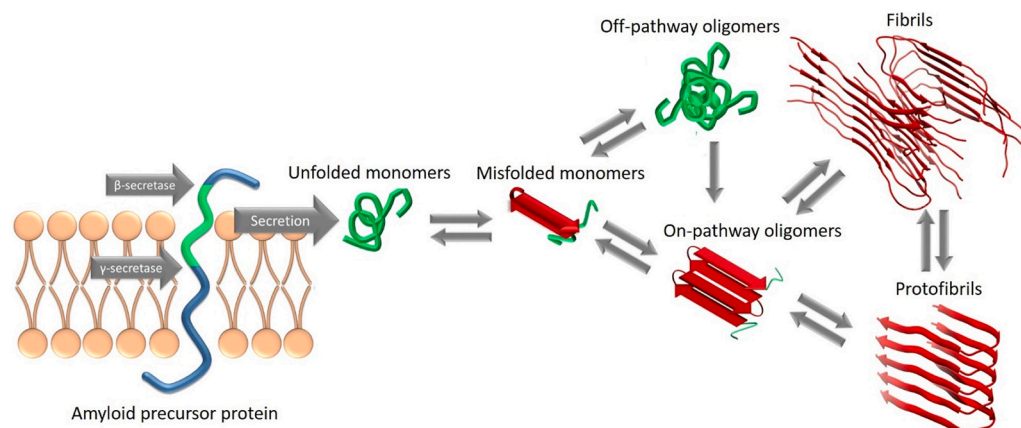


**Fig. 1.** A $\beta$  production via sequential cleavage of the amyloid precursor protein (APP) segment (colored in green) by  $\beta$ -secretase, followed by  $\gamma$ -secretase. After unfolded A $\beta$ M are secreted into the cell environment, they can get misfolded and start aggregating and adopting various conformational states according to different aggregation pathways. The scheme was produced using UCSF Chimera software [21] using PDB files 1Z0Q [22], 2BEG [23], and 2LMN [24] for partially folded monomers/oligomers, protofibrils, and fibrils, respectively. (For interpretation of the references to color in this figure legend, the reader is referred to the web version of this article.)

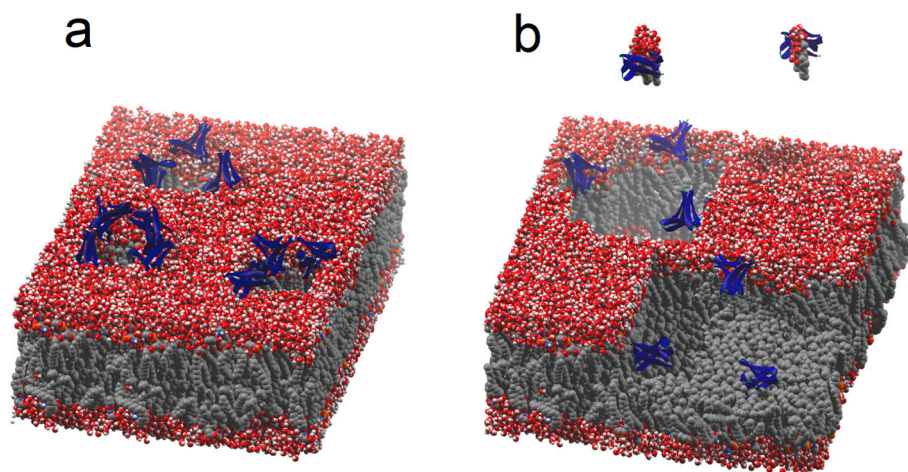


Fig. 2. Lipid bilayer destruction by AβOs via the mechanism of (a) pore formation and (b) lipid extraction.

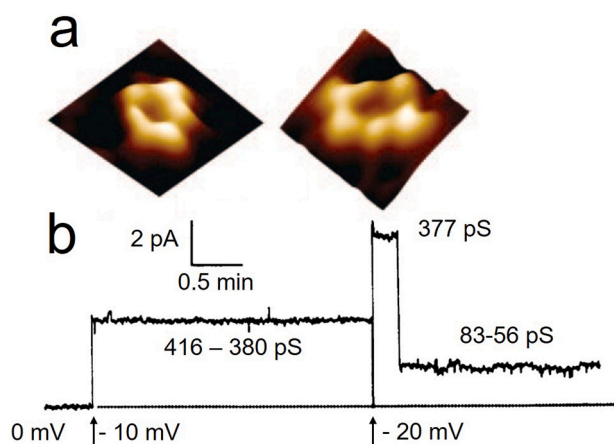


Fig. 3. (a) AFM images of the ion channels formed in the DOPC membrane by Aβ<sub>40</sub>Os [adapted from [39]]. (b) Multiple electrical conductance states of ion channels formed by Aβ<sub>40</sub>Os in the lipid membrane. [Adapted from [72]].

structurally distinctive ionic channels. The differences between the conductivity of these channels result from different aggregation pathways that led to their formation. When fresh Aβ<sub>42</sub>Ms were added to the bilayer, they aggregated on the bilayer surface. Besides, the pre-formed Aβ<sub>42</sub>Os aggregated in the bulk solution before adding them to the lipid bilayer. Lipid bilayers can affect Aβ aggregation (see below). This aggregation might be a reason for the formation of structurally different Aβ<sub>42</sub>Os. Another possibility is that the aggregation pathways of Aβ<sub>42</sub>Ms and Aβ<sub>42</sub>Os were the same, but ion channel-forming Aβ<sub>42</sub>Os in the two cases are produced at different stages of aggregation. However, these two hypotheses are yet to be verified.

The above discussion concludes that Aβ<sub>42</sub>Os can form ion channels in the membrane, while this behavior for Aβ<sub>40</sub>Os is still ambiguous. The effect of membrane composition can be ruled out because the same type of biomimetic system was used in the studies of Aβ<sub>42</sub> and Aβ<sub>40</sub> [69,76]. This conclusion raises a question - what makes Aβ<sub>42</sub>Os more effective in forming ion channels in comparison with Aβ<sub>40</sub>? Aβ<sub>42</sub>Os are more toxic [77,78], and their aggregation pathway is different from that of Aβ<sub>40</sub>Os [79–81]. Aβ<sub>42</sub> contains two other hydrophobic amino acids at C-terminus in comparison with Aβ<sub>40</sub>. Increased hydrophobicity of Aβ<sub>42</sub>Os is correlated with their toxicity. However, the mechanism of this phenomenon is still unknown. There are two possibilities to consider. First, the increased hydrophobicity of Aβ<sub>42</sub>Ms might be the reason for the

formation of structurally unique Aβ<sub>42</sub>Os in solution bulk, that are more capable of forming ion channels compared to Aβ<sub>40</sub>Os. Structural comparison of Aβ<sub>40</sub>Os and Aβ<sub>42</sub>Os produced under identical conditions could confirm or negate this hypothesis. Second, the increased hydrophobicity of Aβ<sub>42</sub>Ms stimulates their interaction with the membrane hydrophobic core that enhances Aβ<sub>42</sub>Ms rearrangement into ion channel-forming Aβ<sub>42</sub>Os. However, this aspect also requires further research to be elucidated.

### 3. Lipid extraction from bilayer lipid membranes

In the mechanism of lipid extraction from bilayer lipid membrane, the toxic peptide binds to lipids and then extracts them from the membrane (Fig. 2b). The AFM study [43] showed distinct interactions of small and large globular Aβ<sub>42</sub>Os with the brain's total lipid extract bilayer (Fig. 4a). Large Aβ<sub>42</sub>Os, with the average diameter and height of ~10 and 3–6 nm, respectively, fibrillated on the lipid bilayer surface without permeating it. Small Aβ<sub>42</sub>Os, with the average diameter and height of ~6 and 1.5–2.5 nm, respectively, permeated lipid bilayer via pore formation followed by lipid extraction. The initial pores differed significantly in shape and size from ion channels, suggesting a different type of Aβ-induced lipid membrane permeabilization. The same lipid extraction mechanism was proposed and named as detergent-like solubilization, membrane dissolution, membrane fragmentation, or lipid uptake by Aβ [41,44–46,82]. High-speed AFM imaging showed the dissolution of a membrane composed of POPC/Chol/SM/GM1 by a mutant form of Aβ<sub>42</sub>Os [82]. The diameter and height of these oligomers were ~17.8 and ~9.6 nm, respectively. Moreover, Aβ<sub>42</sub>Os induced poration and lipid extraction from the lipid bilayer (Fig. 4b), while

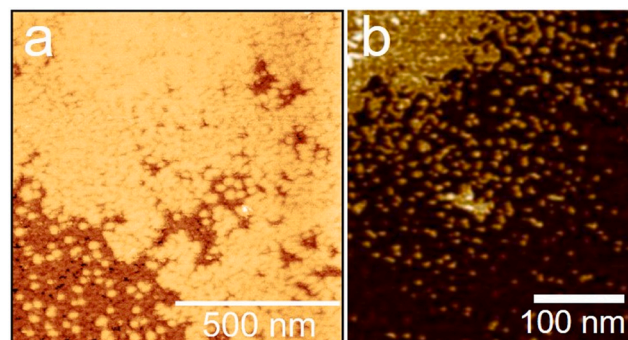


Fig. 4. AFM images of (a) the brain total lipid extract membrane [adapted from [43]] and (b) egg PC/cholesterol/GM1 membrane [adapted from [41]] after lipid extraction by Aβ<sub>42</sub>Os.



A $\beta_{42}$ Ms and A $\beta_{42}$ Fs remained inert towards the membrane [41]. The molecular weight and diameter of these toxic A $\beta_{42}$ O were 30–400 kDa and 10–12 nm, respectively. In agreement with the previously mentioned studies [43,82], the observed pores were significantly larger (~50 nm in diameter) than ion channels (1–2 nm) [39]. Mixing of A $\beta_{40}$ Ms with lipids before vesicle formation (pre-incorporation) leads to the formation of A $\beta$ -lipid complexes because of A $\beta_{40}$ -induced vesicle disruption [44]. The TEM studies showed that only 4-h incubation was required to observe the membrane disruption and formation of short A $\beta_{40}$  protofibrils. Noteworthy, the resolution of the TEM image provided was insufficiently high for resolving smaller aggregates. On the other hand, mixing A $\beta_{40}$ Ms with pre-formed lipid vesicles (external addition) resulted in A $\beta$  fibrillation on the membrane surface after 46 h of incubation but, importantly, without disrupting the membrane. Continuation of this study showed that the pre-incorporated (membrane-disrupting) A $\beta$  forms were rich in  $\beta$ -sheets, while externally added (fibrillating) A $\beta$  forms were unstructured [45,46]. Moreover, they showed that the CH<sub>2</sub> group of lipids interacts with the C $\alpha$  nuclei of Asp23 and Ser26, suggesting that the A $\beta$ -lipid binding in a complex was residue-specific.

Further investigations aimed at explaining the difference in the pre-incorporated and externally added A $\beta_{40}$  interactions with lipid vesicles by monitoring the influence of the peptide-to-lipid (P-to-L) ratio (see discussion in the Lipid membrane properties section, below) [45]. The above studies showed that the ( $\beta$ -sheet)-rich A $\beta$ O permeated the lipid membrane by extracting lipids from the membrane and forming A $\beta$ O-lipid complexes. The resulting pores are the exclusive consequence of A $\beta$ -induced lipid extraction [41]. However, the temporal AFM study showed that, first, A $\beta$ O formed temporary stable pores in the membrane and then clogged them during their incorporation into the membrane core [43]. After that, A $\beta$ O extract lipids from the membrane by forming a complex that diffuses away from the membrane, thus leaving a permanent membrane defect. Still, it is unclear whether the A $\beta$ O-induced lipid extraction mechanism depends on the size of the A $\beta$ O molecules or not. This AFM study shows that large A $\beta_{42}$ O do not permeate the membrane but aggregate on its surface [43]. Contrary to these results, other studies have shown that large A $\beta_{42}$ O permeated the lipid bilayer [41,82]. This contradiction could be explained by invoking different A $\beta$  aggregation pathways caused by different experimental conditions, e.g., using various solvents for breaking pre-existing A $\beta$  aggregates and rendering A $\beta$ Ms, temperature, the buffer solution composition, the ionic strength of the buffer, etc. Moreover, the difference in the lipid composition of the membranes used in these studies could have caused different A $\beta_{42}$ O-membrane interactions. Some studies [41,82] used a simple lipid bilayer composed of 3–4 different lipids, while others [43] used the lipid extract from a porcine brain. The composition of this extract resembles that of a more physiologically-relevant lipid membrane. Studies have shown that lipid composition influences the resulting A $\beta$ -lipid interaction. This effect will be discussed further in the Lipid membrane properties section below [82–86].

#### 4. Non-specific bilayer lipid membrane permeation

Here, we discuss the results of studies on the lipid bilayer permeation by A $\beta$  that do not support any specific permeation mechanism like ion channel/pore formation or lipid extraction mechanism. In these studies, this mechanism is not specified. Therefore, the name of this mechanism is non-specific permeation.

Unlike A $\beta_{42}$ Ms or A $\beta_{42}$ Fs, only A $\beta_{42}$ O permeate lipid bilayers composed of a 1-palmitoyl-2-oleoyl-*sn*-glycero-3-phosphocholine (POPC)/biotinylated POPC mixture [25]. Unfortunately, no details on the secondary structure or size of the studied A $\beta_{42}$  forms were provided. Further research on lipid bilayer permeation mechanism showed that a mixture of monomers and small globular oligomers of a height of 0.5–2.0 nm effectively permeated the POPC/biotinylated POPC lipid bilayer. In comparison, a mixture of globular oligomers and 0.4–1.0 nm

high and several hundred nm long protofilaments caused inflammation of microglia cells [53]. These results suggest that the mechanism of the A $\beta$ O toxicity depends upon these oligomers' size. The activity of small oligomers (lipid bilayer permeation) was inhibited by the antibody that targets C-terminal regions, and the activity of protofilaments (cell inflammation) was hindered by the antibody that targets N-terminal regions. Evidently, C- and N-terminal residues in small oligomers and protofilaments, respectively, were solvent exposed, thus suggesting that significant structural differences between them govern their unique toxic effects. Interactions of small A $\beta$  aggregates extracted from cerebrospinal fluid (CSF) of healthy (control) individuals and large A $\beta$  aggregates extracted from CSF of the mild cognitive impairment (MCI) and AD individuals were studied [54]. MCI is conceptualized as a stage preceding AD [87]. CSF from healthy individuals contained globular aggregates only (Fig. 5a). CSF from MCI and AD individuals consisted of both globular and elongated aggregates (Fig. 5b and c). Importantly, the size of the elongated aggregates present in the CSF from individuals with MCI and AD differed. That is, the elongated aggregates from MCI individuals, termed protofilaments, were 0.3–1.0 nm high and 50–100 nm long. Besides, CSF of AD individuals contained a small fraction of protofilaments and a high population of the 1–3 nm high elongated aggregates, termed protofibrils. The length of both protofilaments and protofibrils characteristic of AD individuals ranged from 50 up to 400 nm. Apparently, protofilaments present in AD individuals are much longer than those present in MCI individuals. This study confirmed the size-dependent difference in the A $\beta$ O toxic actions showing that small aggregates permeate cell membrane (Fig. 5d), while large aggregates induce cell inflammation (Fig. 5f). However, the cell membrane permeation was not associated with globular but with elongated aggregates [54], in contrast to the previous study [53]. The C-terminus targeting antibody inhibited the cell membrane permeation (Fig. 5e). The cell inflammation by protofibrils was inhibited only by the N-terminus targeting antibody (Fig. 5g). In mature fibrils, the N-terminus is exposed while C-terminus is hidden. Therefore, it is inaccessible to the C-terminus active antibodies [88]. This property might explain why the cell inflammation, exerted by large protofibrils, was inhibited only by N-terminus targeting antibody.

It has been demonstrated successfully that small A $\beta$  aggregates permeated the lipid bilayer, while large A $\beta$  aggregates induced cell inflammation. However, it has not been explained why these actions were associated with globular [53] and elongated [54] aggregates, respectively. C-terminal targeting antibodies efficiently inhibit lipid membrane permeabilization by small globular oligomers [53] and small protofilaments [54], indicating that both forms have solvent-exposed C-terminal residues. These results suggest that this permeation is independent of A $\beta$  aggregates shape, but only aggregates with C-terminal residues exposed can exert it. Notably, the N-terminus targeting antibody also inhibits the lipid bilayer permeation though less than the C-terminal targeting antibody [54]. On the other hand, cell inflammation is only observed in the presence of protofibrils with the N-terminal residues exposed. These results indicate that the toxicity mechanism depends on A $\beta$  aggregates' structure, i.e., whether their C- or N-terminal residues are exposed. However, the origin of the exposition of C- and N-terminal residues is under question. There might be two possibilities.

One possibility is that protofilaments and protofibrils are formed by structurally distinct subunits ("seeds") with C- and N-terminal residues exposed. Soluble oligomers' conversion to fibril seeds involves  $\beta$ -strands rotation by 90° [89–91]. In this particular A $\beta_{42}$ O model, the packing of adjacent  $\beta$ -sheets is in a "face-to-back" arrangement with more C-terminal residues exposed, while in A $\beta_{42}$ F, the C-terminal region is buried inside [90]. This model suggests that A $\beta_{42}$ O must convert into fibril seeds that have N-terminal residues exposed to be able to produce elongated structures with exposed N-terminal residues like protofibrils and fibrils. However, this model does not explain the formation of protofilaments with C-terminal residues exposed. Presumably, the globular A $\beta_{42}$ O can also assemble into elongated protofilaments while

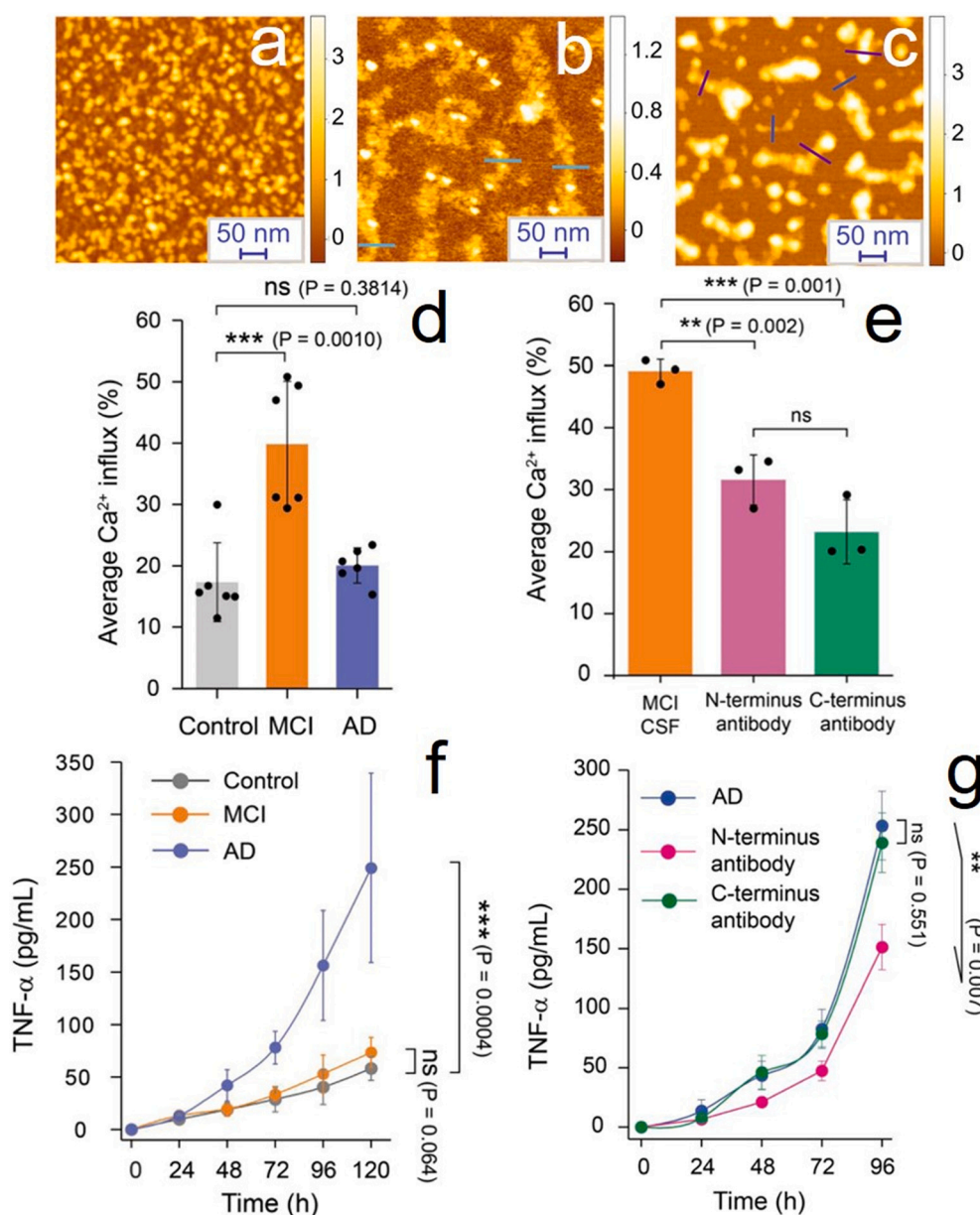


**Fig. 5.** (a–c) AFM images of A $\beta$  aggregates extracted from healthy (control) individuals, as well as individuals with mild cognitive impairment (MCI) and Alzheimer's disease (AD). (d) The membrane permeabilization assay for 16:0–18:1 PC and 18:1–12:0 biotin PC lipid vesicles in the presence of A $\beta$  aggregates extracted from CSF of the control, MCI, and AD individuals. (e) The membrane permeabilization assay for 16:0–18:1 PC and 18:1–12:0 biotin PC lipid vesicles in the presence of A $\beta$  aggregates extracted from CSF of MCI individuals, as well as N- and C-terminus-targeting antibodies. (f) The cell inflammation assay for BV2 cells in the presence of A $\beta$  aggregates extracted from healthy (control) individuals, as well as individuals with MCI and AD. (g) The cell inflammation assay for BV2 cells in the presence of A $\beta$  aggregates extracted from AD individuals, as well as N- and C-terminus-targeting antibodies. [Adapted from [54]].

keeping their C-terminal residues exposed. This hypothesis would explain why membrane permeation is independent of A $\beta$  aggregate shape, i.e., why it is observed for both globular and elongated A $\beta$  aggregates and why it is inhibited by C-terminal targeting antibody. This question remains to be elucidated.

The other possibility is that the intertwining of protofilaments forms the cell-inflaming protofibrils. During this process, the N-terminal residues get exposed, while C-terminal residues get buried. Mature fibrils are composed of intertwined protofilaments [88]. This possibility could explain the formation of protofilaments with exposed C-terminal residues. Moreover, it could elucidate why, in some cases, elongated A $\beta$  aggregates, like A $\beta$ O<sub>s</sub>, permeate lipid membranes.

In any case, one may ask why exposure to different residues generates different toxic actions? One possible explanation is the difference in hydrophobicity of the resulting pathogenic species. The C-terminus of A $\beta$  is highly hydrophobic [66,92], while the N-terminus is hydrophilic [93,94], thus explaining why smaller aggregates are more hydrophobic than larger aggregates. A polar physiological solution is not preferable for the smaller aggregates. Therefore, they permeate the lipid bilayer to

incorporate themselves into the membrane hydrophobic core. On the other hand, large A $\beta$  aggregates have their N-terminal residues exposed, which makes them hydrophilic. Therefore, they do not tend to incorporate into the membrane, and they can stay on the membrane surface. These phenomena may explain not only why A $\beta$ <sub>42</sub>F<sub>s</sub> are considered as non-toxic and cannot permeate lipid bilayers [43], but also the toxicity and membrane-permeating ability of A $\beta$ <sub>42</sub>O<sub>s</sub>.

Many other studies suggest the correlation between A $\beta$ O<sub>s</sub> hydrophobicity and toxicity [56–58]. The increase in surface hydrophobicity of ( $\beta$ -sheet)-rich oligomers of E22G (arctic) A $\beta$ <sub>42</sub>, a variant of A $\beta$ <sub>42</sub>, correlates with the increase in the cell death caused by the cell membrane permeabilization [56]. Moreover, hydrophobicity-dependent and size-independent A $\beta$ <sub>42</sub>O<sub>s</sub> toxicity were demonstrated [57]. For this purpose, two types of A $\beta$ <sub>42</sub>O<sub>s</sub> of similar sizes were produced. These A $\beta$ <sub>42</sub>O<sub>s</sub> revealed different toxicity levels. AFM imaging showed that the height of two kinds of oligomers was ~6.1 nm. Circular dichroism (CD) investigations showed that both types of A $\beta$ <sub>42</sub>O<sub>s</sub> did not contain the  $\beta$ -sheet structure, but they were rich in random coils. However, only oligomers of higher hydrophobicity exhibited toxic activity towards

PC12 cells and increased L- $\alpha$ -phosphocholine lipid bilayers' conductance [57]. This study is not the only one reporting on toxic A $\beta$ O that lack an ordered structure. A $\beta_{42}$ O with both the  $\beta$ -sheet [62–64] and random coil secondary structure exhibit toxicity towards phospholipid membrane [57,65,66]. An amyloid inhibitor, known as K162, binds to hydrophobic residues of small A $\beta_{42}$ O, thus preventing them from permeating the DSPE/POPC/Chol/GM1/SM lipid membrane [95]. Moreover, the K162-induced blockage of A $\beta_{42}$ O hydrophobic residues modifies their aggregation pathway, demonstrating the importance of hydrophobic residues importance in A $\beta$  toxicity and aggregation.

The combinatorial change of hydrophobicity and size of A $\beta_{40}$  aggregates was correlated with their ability to permeate the lipid membrane [58]. The increase in the A $\beta_{40}$  aggregates size and surface hydrophobicity appeared to correlate with increased cellular toxicity and DOPE/DOPS/DOPC membrane permeation. The correlation of large aggregates with increased toxicity agrees with some studies [61] but contradicts the others [26,27,43,53,54,57]. Noteworthy, the size of these aggregates was determined by dynamic light scattering (DLS) measurements. The DLS results can be misleading for heterogeneous samples like A $\beta$  because they show the average size of all aggregates in the sample (not size distribution) [96], and the particle shape is assumed to be spherical, which is not valid for all A $\beta$  aggregates. Therefore, DLS is not a suitable technique for anisotropic polymorphic particles like elongated A $\beta$  forms, and the DLS results should be verified using a different technique [97].

The two studies providing the hypothesis that large aggregates are more toxic [58,61] showed that their aggregates differed in shape, i.e., globular oligomers vs. elongated protofibrils, thus supporting the shape-independent A $\beta$  toxicity. Both the size and shape of A $\beta$  aggregates might depend on the aggregation pathway. The A $\beta$  aggregation can follow different pathways (Fig. 1) [11–19]. Some of those involve the formation of short protofilaments and protofibrils that mutually intertwine to form A $\beta$ Fs. In contrast, A $\beta$ Fs are produced directly by globular oligomers in other pathways. In that way, the formation of protofilaments and protofibrils is bypassed [98,99]. A similar number of monomer subunits can rearrange into aggregates of different sizes and shapes because they follow different aggregation pathways. This inference could explain why many studies indicated A $\beta$ O of various sizes and shapes to be either toxic or non-toxic. One difficulty in establishing the size- and shape-toxicity correlation is the lack of consensus on A $\beta$  aggregates' classification according to their size, molecular weight, and shape. Each research group classifies A $\beta$  aggregates into small and large based on their size measurements. Moreover, it is unclear whether A $\beta$  filaments and protofibrils should be regarded as A $\beta$ O or A $\beta$ F or as a separate aggregate class. Providing an official classification of A $\beta$  aggregates would facilitate comparing published results and determining the size- and shape-toxicity correlation.

As mentioned above, both small, globular A $\beta$ M and large, elongated A $\beta$ Fs are not toxic. On the other hand, intermediate aggregates formed along the aggregation pathway are toxic. This behavior implies that significant structural changes occur at two steps of the aggregation, i.e., during aggregation of A $\beta$ M into toxic A $\beta$ O and conversion of toxic A $\beta$ O into non-toxic A $\beta$ F. First, the transformation of unfolded A $\beta$ M to the ( $\beta$ -sheet)-rich A $\beta$ O occurs. This process may also involve the formation of the intermediate, transiently stable  $\alpha$ -helical A $\beta$ M. Next, rotation of  $\beta$ -strands by 90° leads to the creation of fibril seeds that associate into A $\beta$ Fs [63,89,100]. These results indicate that toxic A $\beta$ O are transiently stable structures that lose their toxicity upon conversion to fibril seeds. However, this conclusion does not explain the formation of toxic A $\beta$ O lacking the  $\beta$ -sheet structure [57,65,66]. Different experimental conditions either stimulate various aggregation pathways or simply render structurally different A $\beta$ M that prefer to follow unique aggregation pathways. In both cases, these different aggregation pathways would produce toxic A $\beta$  aggregates of different shapes, sizes, and secondary structures, thus making the size- and shape-toxicity correlation challenging. However, to the best of the authors' knowledge, no

study shows toxic A $\beta$  aggregates that are not hydrophobic. This inference suggests that the critical moment for A $\beta$  toxicity along any aggregation pathway is when the aggregates with the highest surface hydrophobicity are formed. These aggregates might have different shapes, sizes, secondary structures and be formed at different points in time, depending on the aggregation pathway. This hypothesis would explain the conflicting results of the studies showing toxic A $\beta$ O of different shapes, sizes, and secondary structures.

## 5. Bilayer lipid membrane properties

Lipid rafts are cell membrane domains enriched in sphingolipids, glycolipids, and cholesterol [101]. Alterations in the lipid rafts are associated with neuronal loss and neurodegeneration [102]. Therefore, it is interesting to understand how changes in the composition of the lipid raft-mimicking membranes affect their interaction with A $\beta$ .

Toxicity of mutant A $\beta_{42}$  (MA $\beta$ ) peptide, in which cysteine replaces glycine as the 37th residue, was studied [82,83]. A high-speed AFM imaging showed that MA $\beta$  formed oligomers (MA $\beta$ O) with average diameter and height of ~20 and ~10 nm, respectively [82]. These MA $\beta$ O are very stable and do not aggregate into A $\beta$ Fs. Interaction of MA $\beta$ O with lipid bilayers of different lipid compositions was studied [82]. MA $\beta$ O were inactive towards a bilayer composed of sphingomyelin, POPC, and cholesterol. Replacement of cholesterol with GM1 in the bilayer resulted in MA $\beta$ O adsorption on the bilayer surface, but the bilayer integrity remained preserved. Adding both cholesterol and GM1 into the lipid bilayer resulted in membrane destruction via the MA $\beta$ O-induced lipid extraction mechanism. Other studies demonstrated that only cholesterol is necessary for MA $\beta$ O binding to the lipid bilayer [83]. Interactions of MA $\beta$  monomers (MA $\beta$ M) and MA $\beta$ O, as well as two other A $\beta_{42}$  variants, with lipid membranes were compared [103]. Interestingly, both MA $\beta$ M and MA $\beta$ O permeated the DOPG but not DOPC vesicles. It might seem surprising that the negatively charged A $\beta_{42}$  exhibits affinity to negatively charged lipids higher than to zwitterionic lipids. However, this higher affinity has already been demonstrated [104–107]. The reason for this phenomenon is the hydrogen bonding of A $\beta_{42}$  side chains with the surface-exposed OH groups in the heads of DOPG rather than electrostatic interaction. Moreover, this kind of interaction was also proposed to account for A $\beta$  binding with gangliosides, also rich in OH groups [105,108]. A $\beta_{42}$  aggregation was significantly accelerated by increasing the cholesterol content in the DMPC and DMPC/DMPE vesicles (Fig. 6) [86]. These results indicate that the interaction of A $\beta$  with lipid membranes depends on the lipid composition even though the respective conclusions drawn on the role of cholesterol are ambiguous, i.e., whether A $\beta$  binds to cholesterol-containing membranes or not [82,83].

Some studies disagreed with the weak binding of A $\beta_{42}$  to zwitterionic lipids [109–111]. For instance, they claim that, initially,  $\alpha$ -helical A $\beta_{40}$ M not only bind but also perturb the POPC bilayer while changing its structure to  $\beta$ -sheet [109]. Moreover, they induced spiky, fast cation channels in the POPC/POPE membranes. A $\beta_{42}$  incurred perturbation in both the genuine POPC and POPC/sphingomyelin/cholesterol vesicles [110]. Interestingly, DLPC vesicles inhibited A $\beta_{40}$  aggregation by stabilizing unstructured aggregates that disrupted both DLPC vesicles and bilayers via the lipid extraction mechanism [111]. On the other hand, the DOPC and POPC membranes accelerated A $\beta_{40}$  aggregation, and after 24 h ( $\beta$ -sheet)-rich fibrils were formed.

Remarkably, DLPC can remodel pre-formed A $\beta_{40}$ F. This remodeling leads to the formation of thin fibrils incapable of binding to the thioflavin T (ThT) dye, despite their  $\beta$ -sheet secondary structure typical of A $\beta_{40}$ Fs [111]. Presumably, the DLPC-remodeled A $\beta_{40}$ Fs have a  $\beta$ -sheet secondary structure, in which DLPC lipids occupy the ThT binding sites. However, this speculation remains to be confirmed. Moreover, A $\beta_{40}$ M either perturb the POPC membrane [109] or aggregate on the POPC membrane without permeating it [111]. Most likely, this contradiction arises from different sample preparation procedures adopted in these



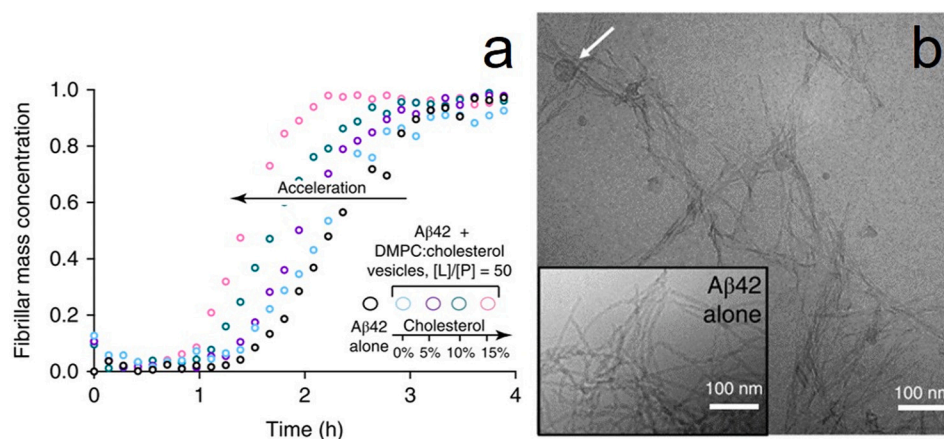


**Fig. 6.** (a) Kinetic profiles, based on the thioflavin T (ThT) dye fluorescence assay, for the Aβ<sub>42</sub> aggregation in the presence of either DMPC or DMPC/cholesterol vesicles containing increasing concentrations of cholesterol up to 15%. (b) TEM images of Aβ<sub>42</sub>Fs formed in the (inset) absence or presence of DMPC/cholesterol vesicles containing 15% of cholesterol. The arrow points towards DMPC/cholesterol vesicles. [Adapted from [86]].

two studies. In both studies, the Aβ concentration and P-to-L ratio were varied depending on the kind of measurement performed. The Aβ aggregation rate depends on the Aβ concentration. Therefore, it is essential to keep the Aβ concentration and P-to-L ratio constant to supplement all measurements' results.

The catalytic effect of cholesterol-containing vesicles on Aβ<sub>42</sub> aggregation was studied [86]. The lipid vesicles used were composed of lipids with PC heads and acyl chains of different lengths and degrees of unsaturation. It appeared that the Aβ<sub>42</sub> aggregation rate was higher, the higher was the degree of unsaturation in lipids (DMPC < POPC < DOPC) [86]. This effect was attributed to the increased bulkiness and exposure of acyl chains in unsaturated lipids. Additionally, the lipid vesicle size did not impact the Aβ<sub>42</sub> aggregation rate. The initially disordered globular Aβ<sub>42</sub> formed (β-sheet)-rich fibrils after 12 h of aggregation. The ThT fluorescence analysis confirmed that the increase in the P-to-L ratio accelerated the Aβ<sub>42</sub> aggregation [86]. Evidently, a relative lipid concentration increase leads to the acceleration of the aggregation.

Some studies highlighted the significance of electrostatic interaction of charged parts of lipids with Aβ. [105–107]. Variations in the Aβ/lipid vesicle solution's pH incurred variations in electrostatic interaction of AβMs with DOTAP and egg yolk PG lipids [105]. This phenomenon was absent for the lipid raft mimicking a membrane composed of cholesterol, sphingomyelin, and GM1. The electrostatic interaction of AβMs with lipid monolayers could range from strongly attractive (Aβ-DPTAP in PBS), through moderately attractive (Aβ-DPPG and Aβ-DPPC in water), to strongly repulsive (Aβ-DPPG in PBS) [106]. The change in the peptide charge and charge screening effects, adjusted by the appropriate change of pH and ionic strength of the solution, respectively, leads to the change in the strength of the interaction between AβMs and lipids because of its electrostatic nature. The increase in the bilayer negative surface charge, caused by the increase in the content of DMPG in the DMPC/DMPG mixture, leads to the increase in the amount of (β-sheet)-rich Aβ<sub>40</sub> bound to the membrane surface [107]. Apparently, electrostatic attraction of positively charged Aβ<sub>40</sub> residues (Arg5, Lys16, and Lys28) and negatively charged lipid heads is essential. The electrostatic interaction occurred for Aβ<sub>40</sub>Ms externally added to the pre-formed lipid vesicles. Interestingly, the C-terminal hydrophobic part of the peptide was inserted in the membrane when Aβ<sub>40</sub>Ms were pre-mixed with lipids before they formed vesicles [107]. In this case, the increase in the anionic lipid content leads to electrostatic anchoring of charged Aβ<sub>40</sub> residues with lipid heads, thus stimulating further insertion of the hydrophobic peptide segments into the membrane and increasing the content of the α-helical secondary structure.

GM1 is an essential component of lipid rafts present in neuronal

membranes. It influences Aβ-lipid membrane interaction [85,112]. Increasing the GM1 content in the cell membrane increases the Aβ<sub>42</sub>Os association on the membrane surface, thus enhancing the Ca<sup>2+</sup> transfer across the cell membrane [85]. However, a decrease in the GM1 concentration decreases this neurotoxic effect. This toxicity can be inhibited by blocking GM1 interaction with Aβ<sub>42</sub>Os with Cholera Toxin Subunit-B. This blocking can evidence the importance of GM1 in the Aβ<sub>42</sub>Os toxicity. The supported DMPC bilayers and vesicles perturbation by Aβ<sub>40</sub>Os is enhanced in the presence of GM1 [112]. This Aβ<sub>40</sub>Os-lipid interaction results in the formation of hexagonal micelles. Moreover, the presence of GM1 influences the insertion of Aβ<sub>40</sub>Ms into the DPPC/GM1 monolayer [113]. At low GM1 concentration, Aβ<sub>40</sub> disrupts the membrane morphology, thus causing expansion of the fluid phase.

In contrast, Aβ<sub>40</sub> disrupts both the fluid and condensed domains (gel phase) at high GM1 concentrations. Variation in pH and ionic strength of water solutions may enhance either strong attractive or repulsive Aβ-GM1 interaction, thus indicating that the interaction is driven electrostatically. Surprisingly, the incubation of Aβ<sub>40</sub> with POPC/GM1 vesicles resulted in Aβ fibrillation [113]. Why does GM1 stimulate disruption of DPPC monolayers by Aβ<sub>40</sub>, while when being incorporated into POPC vesicles, it enhances Aβ fibrillation? One possible explanation originates from the difference in the Aβ<sub>40</sub> concentrations employed in the two experiments. In the experiments involving DPPC monolayers, the Aβ<sub>40</sub> concentration was 250 nM, while in experiments with POPC vesicles, it was 100 μM. However, whether this was the cause of the discrepancy remains to be elucidated.

Some studies suggest that Aβ<sub>40</sub> interaction with lipid vesicles is independent of lipid composition, but the P-to-L ratio influences it [114]. At a high P-to-L ratio, the Aβ<sub>40</sub> was converted from the α-helix to the β-sheet secondary structure within 4 h, and neither protofibrils nor fibrils were formed. Only the (β-sheet)-rich Aβ<sub>40</sub>Os, which induced the membrane content leakage, were formed during this time frame. At a low P-to-L ratio, the peptide's structural conversion from α-helix to the random coil was accompanied by the formation of off-pathway Aβ<sub>40</sub>Os. These Aβ<sub>40</sub>Os stimulated the mixing of lipid molecules between neighboring lipid vesicles, thus resulting in their fusion. Other studies by the same group [45,115] associated a low P-to-L ratio with the same lipid mixing/vesicle fusion mechanism. However, in these cases, the same mechanism was associated with Aβ<sub>40</sub>Ms, not with off-pathway Aβ<sub>40</sub>Os, as in the previous study [114]. Interestingly, both the off-pathway Aβ<sub>40</sub>Os from the former study [114] and the Aβ<sub>40</sub>Ms from the latter [45,115], that induced lipid mixing/vesicle fusion, were unstructured, i. e., they had a high content of the random coil secondary structure. On the other hand, (β-sheet)-rich Aβ<sub>40</sub>Os from the previous study [114]

induced leakage of the membrane content. Therefore, these studies suggest that different A $\beta$ -lipid interactions result from different A $\beta$  secondary structures and a P-to-L ratio. However, these results contradict previous studies showing that unstructured A $\beta$ O<sub>s</sub> could also permeate lipid membranes [57,65,66]. Therefore, this rules out the secondary structure of A $\beta$ O<sub>s</sub> as a factor determining the A $\beta$ -lipid interaction. However, this and other studies strongly indicate that the A $\beta$ -lipid interaction is affected by the P-to-L ratio [45,86,114,115]. The overall conclusion is that a low P-to-L ratio facilitates A $\beta$  aggregation, and a high P-to-L ratio facilitates permeation of the lipid membrane by A $\beta$  aggregates. It would be essential to find the threshold value of the P-to-L ratio determining the border between these two processes. Determining the P-to-L ratio value at which the membrane starts decomposing would unravel the A $\beta$  concentration on the membrane surface that is lethal to the cell.

## 6. Novel hypotheses

The correlation of the A $\beta$  toxicity at early aggregation stages with membrane damage has also been explained by another mechanism, called a “lipid-chaperone” hypothesis [116,117]. According to this hypothesis, freely-dispersed phospholipids, which are in chemical equilibrium with their supramolecular assemblies (micelles, vesicles, and bilayer), play a key role in the formation of lipid-peptide complexes. These complexes facilitate A $\beta$  insertion into the membrane. Therefore, free phospholipids act as chaperones to insert A $\beta$  into the membrane.

The presence of lipid-A $\beta$  complexes was confirmed by both biophysical (2D NMR spectroscopy, CD spectroscopy, and isothermal titration calorimetry (ITC) measurements) and theoretical (molecular dynamics, MD, simulations) methods [117,118]. Notably, the lipid-A $\beta$  complex formation competes with A $\beta$  oligomerization. Therefore, the change of the free lipid content in the solution affects the A $\beta$  aggregation. The free lipid concentration is characterized by the critical micellar concentration (CMC), which depends on the lipid alkyl chain length and the lipid head charge [119]. Free lipids form stable peptide-lipid complexes with hydrophobic A $\beta$  monomers [117]. At high CMC (phospholipids with short alkyl chains), the formation of A $\beta$  fibrils is suppressed, and ion-channel-like pores are formed by A $\beta$ -lipid complexes in the phospholipid bilayer (Fig. 7). In contrast, at low CMC (phospholipids with long alkyl chains), the fibril formation is facilitated, and A $\beta$  fibrils destroy the membrane according to the detergent-like mechanisms

(Fig. 7). At intermediate CMC values, both mechanisms are feasible.

Furthermore, the A $\beta$  interaction with the membrane, through both ion-channel-like and detergent-like mechanisms, is more effective in the presence of free phospholipids in solution. That is because the lipid-A $\beta$  complex is more hydrophobic than the bare A $\beta$ . That may suggest that the lipid-A $\beta$  complex formation is required for A $\beta$  penetration into the lipid bilayer while the CMC value discriminates between ion-channel-like pore formation, detergent-like mechanism, and fibril formation in the aqueous phase [117].

NMR and CD spectroscopy studies showed that the free DMPC monomers' interaction with A $\beta$ <sub>40</sub> induces conformational changes in these peptides [117]. This interaction is predominantly hydrophobic. It involves specific A $\beta$  amino acid segments enriched with hydrophobic residues and lipids alkyl chains. A $\beta$ <sub>40</sub> monomers, in the absence of free lipids, are characterized by a disordered secondary structure that changes into  $\beta$ -sheets, indicating peptide aggregation and fibril formation. In contrast, the presence of free DMPC monomers causes A $\beta$ <sub>40</sub> to be characterized by an  $\alpha$ -helix structure. Moreover, the longer the lipid alkyl chains and the higher the  $\alpha$ -helix content of A $\beta$ , the more selective and stronger the lipid-A $\beta$  interaction. Apparently, hydrophobic interactions, enhanced upon  $\alpha$ -helix peptide folding, are the reason for the stable lipid-A $\beta$  complex formation. Interestingly, all-atom molecular dynamics simulations of the complex formation between individual POPC and DPPC and A $\beta$ <sub>42</sub> showed that the A $\beta$  remained largely disordered in 1:1 complexes [118]. However, the lipid-A $\beta$  interaction reduced both peptide flexibility and solvent accessibility. Furthermore, these complexes adsorbed on the membrane surface instead of being incorporated into the membrane. Adding two additional phospholipid molecules to the system caused the A $\beta$  structure to change from disordered to ordered helical or  $\beta$ -sheet because of the hydrophobic interaction between A $\beta$  and the lipid tails. As a result, the formed complex preferentially inserts into the membrane.

One should also mention the symmetry-breaking theory, the theoretical model describing the symmetry-breaking of oligomeric aggregates forming an alternating system of partially ordered and disordered monomers [120,121]. This model predicts the conformational changes in the transition from monomers to larger oligomers. The occurrence of small-scale patterns of alternating ordered and disordered arrangements may provide a new rationale for the molecular origin of fibril polymorphism, as well as the lack of short-range molecular ordering in mature fibrils.

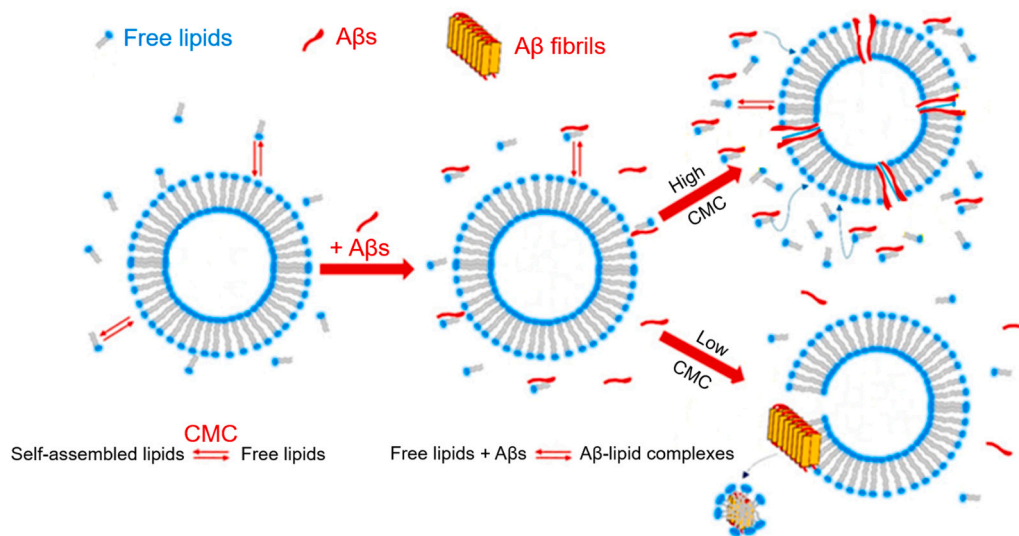


**Fig. 7.** The A $\beta$  interaction with a model membrane in the presence of free monomeric lipids, according to the lipid-chaperone hypothesis. CMC stands for the critical micellar concentration.

[Adapted from [117]].



Both the lipid-chaperone hypothesis and the symmetry-breaking theory are exciting and perspective. However, these hypotheses are quite new, and the experimental data supporting them are still scarce. Undoubtedly, introducing more realistic models to study the influence of cholesterol or surface-exposed sugar groups of gangliosides on the formation of lipid-A $\beta$  complexes and their interaction with the membrane might provide fascinating findings. Noteworthy, even though it is a very novel hypothesis, the lipid-chaperone hypothesis also indicates that A $\beta$  hydrophobicity might be a crucial feature that governs A $\beta$  toxicity and aggregation.

## 7. Summary and outlook

A $\beta$  can exhibit different types of cellular toxicity, and its preference for one toxic mechanism over the other is still unknown. Undoubtedly, A $\beta$ O<sub>6</sub> are the most toxic A $\beta$  form. However, A $\beta$ O<sub>6</sub> of various sizes, shapes, and secondary structures were shown to be toxic (and non-toxic), thus preventing us from reaching a definite conclusion on the A $\beta$ O<sub>6</sub>'s property essential for their toxicity.

To the best of the authors' knowledge, no literature evidences the toxic action of A $\beta$ O<sub>6</sub> with low surface hydrophobicity. This fact prompts a conclusion that surface hydrophobicity is the toxicity-defining property. This feature could explain not only the higher toxicity of A $\beta$ <sub>42</sub> compared to that of A $\beta$ <sub>40</sub> but also the A $\beta$ O<sub>6</sub>'s preference for incorporation into the cell membrane and subsequent membrane permeation. However, A $\beta$  can also aggregate on the membrane surface. It is unclear why A $\beta$  either permeates the cell membrane or fibrillates on its surface. The lipid-chaperone hypothesis indicates that the chemical equilibrium between the free and the membrane phospholipids governs the A $\beta$  transport into the core of the bilayer [5]. Other studies indicate that A $\beta$  preference towards membrane permeabilization or fibrillation also depends upon the lipid composition of the membrane [82,83,109–111], as well as the P-to-L ratio [45,86,114,115], thus revealing the influence of lipids on A $\beta$  behavior. Therefore, future research should be directed towards a deeper understanding of A $\beta$  structural changes responsible for variations in hydrophobicity levels and toxicity. This knowledge would contribute to the development of proper therapeutics for AD. Moreover, it remains to be determined how different phospholipids at different P-to-L ratios affect A $\beta$  behavior. This information would provide us with the critical concentration of A $\beta$  on the membrane surface above which A $\beta$  becomes toxic and could be used for devising AD diagnosis sensors.

## Declaration of competing interest

The authors declare no conflict of interests.

## Acknowledgments

P.P. acknowledges the support of the Polish National Science Centre, grant No. OPUS12 2016/23B/ST4/02791. The research activity of D. M. was supported by funds from the European Union's Horizon 2020 research and innovation program under the Marie Skłodowska-Curie grant agreement No. 711859 and by financial resources for science in the years 2017–2021 awarded by the Polish Ministry of Science and Higher Education for the implementation of an international co-financed project. J.L. acknowledges the support of the Natural Sciences and Engineering Research Council of Canada (NSERC) grant (RG-03958).

## References

- [1] A. Alzheimer, Über eine eigenartige Erkrankung der hirnrinde, *Allg. Z. Psychiatr. Psych. Med.* (1907) 146–148.
- [2] J. Hardy, D.J. Selkoe, The amyloid hypothesis of Alzheimer's disease: progress and problems on the road to therapeutics, *Science* (80-) 297 (2002) 353–356, <https://doi.org/10.1126/science.1072994>.

- [3] D.J. Selkoe, J. Hardy, The amyloid hypothesis of Alzheimer's disease at 25 years, *EMBO Mol. Med.* 8 (2016) 595–608, <https://doi.org/10.15252/emmm.201606210>.
- [4] R.J. O'Brien, P.C. Wong, Amyloid precursor protein processing and Alzheimer's disease, *Annu. Rev. Neurosci.* 34 (2011) 185–204, <https://doi.org/10.1146/annurev-neuro-061010-113613>.
- [5] R. Vassar, B.D. Bennett, S. Babu-Khan, S. Kahn, E.A. Mendiaz, P. Denis, D. B. Teplow, S. Ross, P. Amarante, R. Loeloff, Y. Luo, S. Fisher, J. Fuller, S. Edenson, J. Lile, M.A. Jarosinski, A.L. Biere, E. Curran, T. Burgess, J.-C. Louis, F. Collins, J. Treanor, G. Rogers, M. Citron,  $\beta$ -Secretase cleavage of Alzheimer's amyloid precursor protein by the transmembrane aspartic protease BACE, *Science* (80-) 286 (1999), <https://doi.org/10.1126/science.286.5440.735>, 735 LP – 741.
- [6] A. Bernabeu-Zornoza, R. Coronel, C. Palmer, M. Monteagudo, A. Zambrano, I. Liste, Physiological and pathological effects of amyloid- $\beta$  species in neural stem cell biology, *Neural Regen. Res.* 14 (2019) 2035, <https://doi.org/10.4103/1673-5374.262571>.
- [7] C.M. Dobson, A. Šali, M. Karplus, Protein folding: a perspective from theory and experiment, *Angew. Chem. Int. Ed.* 37 (1998) 868–893, [https://doi.org/10.1002/\(SICI\)1521-3773\(19980420\)37:7<868::AID-ANIE868>3.0.CO;2-H](https://doi.org/10.1002/(SICI)1521-3773(19980420)37:7<868::AID-ANIE868>3.0.CO;2-H).
- [8] J. Bradbury, Chaperones: keeping a close eye on protein folding, *Lancet* 361 (2003) 1194–1195, [https://doi.org/10.1016/S0140-6736\(03\)12975-3](https://doi.org/10.1016/S0140-6736(03)12975-3).
- [9] T.K. Chaudhuri, S. Paul, Protein-misfolding diseases and chaperone-based therapeutic approaches, *FEBS J.* 273 (2006) 1331–1349, <https://doi.org/10.1111/j.1742-4658.2006.05181.x>.
- [10] F.U. Hartl, Protein misfolding diseases, *Annu. Rev. Biochem.* 86 (2017) 21–26, <https://doi.org/10.1146/annurev-biochem-061516-044518>.
- [11] S.I.A. Cohen, R. Cukalevski, T.C.T. Michaels, A. Šarić, M. Törnquist, M. Vendruscolo, C.M. Dobson, A.K. Buell, T.P.J. Knowles, S. Linse, Distinct thermodynamic signatures of oligomer generation in the aggregation of the amyloid- $\beta$  peptide, *Nat. Chem.* 10 (2018) 523–531, <https://doi.org/10.1038/s41557-018-0023-x>.
- [12] D.M. Walsh, A. Lomakin, G.B. Benedek, M.M. Condron, D.B. Teplow, Amyloid  $\beta$ -protein fibrillogenesis, *J. Biol. Chem.* 272 (1997) 22364–22372, <https://doi.org/10.1074/jbc.272.35.22364>.
- [13] S.M. Butterfield, H.A. Lashuel, Amyloidogenic protein-membrane interactions: mechanistic insight from model systems, *Angew. Chem. Int. Ed.* 49 (2010) 5628–5654, <https://doi.org/10.1002/anie.200906670>.
- [14] W.M. Tay, D. Huang, T.L. Rosenberry, A.K. Paravastu, The Alzheimer's amyloid- $\beta$ (1–42) peptide forms off-pathway oligomers and fibrils that are distinguished structurally by intermolecular organization, *J. Mol. Biol.* 425 (2013) 2494–2508, <https://doi.org/10.1016/j.jmb.2013.04.003>.
- [15] T. Watanabe-Nakayama, K. Ono, M. Itami, R. Takahashi, D.B. Teplow, M. Yamada, High-speed atomic force microscopy reveals structural dynamics of amyloid  $\beta$  1–42 aggregates, *Proc. Natl. Acad. Sci.* 113 (2016) 5835–5840, <https://doi.org/10.1073/pnas.1524807113>.
- [16] P. Arosio, T.P.J. Knowles, S. Linse, On the lag phase in amyloid fibril formation, *Phys. Chem. Chem. Phys.* 17 (2015) 7606–7618, <https://doi.org/10.1039/C4CP05563B>.
- [17] B. Mannini, F. Chiti, Chaperones as suppressors of protein misfolded oligomer toxicity, *Front. Mol. Neurosci.* 10 (2017) 98–106, <https://doi.org/10.3389/fnmol.2017.00098>.
- [18] A. Sandberg, L.M. Luheshi, S. Sollvander, T. Pereira de Barros, B. Macao, T.P. J. Knowles, H. Biverstal, C. Lendel, F. Ekholm-Pettersson, A. Dubnovitsky, L. Lannfelt, C.M. Dobson, T. Hardt, Stabilization of neurotoxic Alzheimer amyloid- $\beta$  oligomers by protein engineering, *Proc. Natl. Acad. Sci.* 107 (2010) 15595–15600, <https://doi.org/10.1073/pnas.1001740107>.
- [19] F. Chiti, C.M. Dobson, Protein misfolding, functional amyloid, and human disease, *Annu. Rev. Biochem.* 75 (2006) 333–366, <https://doi.org/10.1146/annurev.biochem.75.101304.123901>.
- [20] T.C.T. Michaels, A. Šarić, S. Curk, K. Bernfur, P. Arosio, G. Meisl, A.J. Dear, S.I. A. Cohen, C.M. Dobson, M. Vendruscolo, S. Linse, T.P.J. Knowles, Dynamics of oligomer populations formed during the aggregation of Alzheimer's A $\beta$ 42 peptide, *Nat. Chem.* 12 (2020) 445–451, <https://doi.org/10.1038/s41557-020-0452-1>.
- [21] E.F. Pettersen, T.D. Goddard, C.C. Huang, G.S. Couch, D.M. Greenblatt, E. C. Meng, T.E. Ferrin, UCSF chimera-a visualization system for exploratory research and analysis, *J. Comput. Chem.* 25 (2004) 1605–1612, <https://doi.org/10.1002/jcc.20084>.
- [22] S. Tomaselli, V. Esposito, P. Vangone, N.A.J. van Nuland, A.M.J.J. Bonvin, R. Guerrini, T. Tancredi, P.A. Temussi, D. Picone, The  $\alpha$ -to- $\beta$  conformational transition of Alzheimer's A $\beta$ (1–42) peptide in aqueous media is reversible: a step by step conformational analysis suggests the location of  $\beta$  conformation seeding, *ChemBioChem.* 7 (2006) 257–267, <https://doi.org/10.1002/cbic.200500223>.
- [23] T. Luhrs, C. Ritter, M. Adrian, D. Riek-Loher, B. Bohrmann, H. Döbeli, D. Schubert, R. Riek, 3D structure of Alzheimer's amyloid- $\beta$ (1–42) fibrils, *Proc. Natl. Acad. Sci.* 102 (2005) 17342–17347, <https://doi.org/10.1073/pnas.0506723102>.
- [24] A.K. Paravastu, R.D. Leapman, W.-M. Yau, R. Tycko, Molecular structural basis for polymorphism in Alzheimer's -amyloid fibrils, *Proc. Natl. Acad. Sci.* 105 (2008) 18349–18354, <https://doi.org/10.1073/pnas.0806270105>.
- [25] P. Flagmeier, S. De, D.C. Wirthensohn, S.F. Lee, C. Vincke, S. Muyldermans, T.P. J. Knowles, S. Gandhi, C.M. Dobson, D. Klenerman, Ultrasensitive measurement of ca<sup>2+</sup> influx into lipid vesicles induced by protein aggregates, *Angew. Chem. Int. Ed.* 56 (2017) 7750–7754, <https://doi.org/10.1002/anie.201700966>.
- [26] K. Ono, M.M. Condron, D.B. Teplow, Structure-neurotoxicity relationships of amyloid  $\beta$ -protein oligomers, *Proc. Natl. Acad. Sci.* 106 (2009) 14745–14750, <https://doi.org/10.1073/pnas.0905127106>.

- [27] P. Cizas, R. Budvytyte, R. Morkuniene, R. Moldovan, M. Broccio, M. Lösche, G. Niaura, G. Valincius, V. Borutaite, Size-dependent neurotoxicity of  $\beta$ -amyloid oligomers, *Arch. Biochem. Biophys.* 496 (2010) 84–92, <https://doi.org/10.1016/j.abb.2010.02.001>.
- [28] E.N. Cline, M.A. Bicca, K.L. Viola, W.L. Klein, The amyloid- $\beta$  oligomer hypothesis: beginning of the third decade, *J. Alzheimers Dis.* 64 (2018) S567–S610, <https://doi.org/10.3233/JAD-179941>.
- [29] G.M. Shankar, S. Li, T.H. Mehta, A. Garcia-Munoz, N.E. Shepardson, I. Smith, F. M. Brett, M.A. Farrell, M.J. Rowan, C.A. Lemere, C.M. Regan, D.M. Walsh, B. L. Sabatini, D.J. Selkoe, Amyloid- $\beta$  protein dimers isolated directly from Alzheimer's brains impair synaptic plasticity and memory, *Nat. Med.* 14 (2008) 837–842, <https://doi.org/10.1038/nm1782>.
- [30] P.N. Mc Donald, G.M. Savva, C. Brayne, A.T. Welzel, G. Forster, G.M. Shankar, D. J. Selkoe, P.G. Ince, D.M. Walsh, The presence of sodium dodecyl sulphate-stable A $\beta$  dimers is strongly associated with alzheimer-type dementia, *Brain* 133 (2010) 1328–1341, <https://doi.org/10.1093/brain/awq065>.
- [31] G.M. Shankar, B.L. Bloodgood, M. Townsend, D.M. Walsh, D.J. Selkoe, B. L. Sabatini, Natural oligomers of the alzheimer amyloid- protein induce reversible synapse loss by modulating an NMDA-type glutamate receptor-dependent signaling pathway, *J. Neurosci.* 27 (2007) 2866–2875, <https://doi.org/10.1523/JNEUROSCI.4970-06.2007>.
- [32] P.N. Lacor, M.C. Buniel, P.W. Furlow, A. Sanz Clemente, P.T. Velasco, M. Wood, K.L. Viola, W.L. Klein, A oligomer-induced aberrations in synapse composition, shape, and density provide a molecular basis for loss of connectivity in Alzheimer's disease, *J. Neurosci.* 27 (2007) 796–807, <https://doi.org/10.1523/JNEUROSCI.3501-06.2007>.
- [33] G. Kroemer, M. Jäättelä, Lysosomes and autophagy in cell death control, *Nat. Rev. Cancer* 5 (2005) 886–897, <https://doi.org/10.1038/nrc1738>.
- [34] S. Rosales-Corral, D. Acuna-Castroviejo, D.X. Tan, G. López-Armas, J. Cruz-Ramos, R. Muñoz, V.G. Melnikov, L.C. Manchester, R.J. Reiter, Accumulation of exogenous amyloid- $\beta$  peptide in hippocampal mitochondria causes their dysfunction: a protective role for melatonin, *Oxidative Med. Cell. Longev.* 2012 (2012) 1–15, <https://doi.org/10.1155/2012/843649>.
- [35] M. Domínguez-Prieto, A. Velasco, A. Taberero, J.M. Medina, Endocytosis and transcytosis of amyloid- $\beta$  peptides by astrocytes: a possible mechanism for amyloid- $\beta$  clearance in Alzheimer's disease, *J. Alzheimers Dis.* 65 (2018) 1109–1124, <https://doi.org/10.3233/JAD-180332>.
- [36] T. Tomiyama, S. Matsuyama, H. Iso, T. Umeda, H. Takuma, K. Ohnishi, K. Ishibashi, R. Teraoka, N. Sakama, T. Yamashita, K. Nishitsuji, K. Ito, H. Shimada, M.P. Lambert, W.L. Klein, H. Mori, A mouse model of amyloid oligomers: their contribution to synaptic alteration, abnormal tau phosphorylation, glial activation, and neuronal loss in vivo, *J. Neurosci.* 30 (2010) 4845–4856, <https://doi.org/10.1523/JNEUROSCI.5825-09.2010>.
- [37] M.T. Ferretti, M.A. Bruno, A. Ducatenzeiler, W.L. Klein, A.C. Cuello, Intracellular A $\beta$ -oligomers and early inflammation in a model of Alzheimer's disease, *Neurobiol. Aging* 33 (2012) 1329–1342, <https://doi.org/10.1016/j.neurobiolaging.2011.01.007>.
- [38] N. Arispe, E. Rojas, H.B. Pollard, Alzheimer disease amyloid beta protein forms calcium channels in bilayer membranes: blockade by tromethamine and aluminum, *Proc. Natl. Acad. Sci.* 90 (1993) 567–571, <https://doi.org/10.1073/pnas.90.2.567>.
- [39] A. Quist, I. Doudevski, H. Lin, R. Azimova, D. Ng, B. Frangione, B. Kagan, J. Ghiso, R. Lal, Amyloid ion channels: a common structural link for protein-misfolding disease, *Proc. Natl. Acad. Sci.* 102 (2005) 10427–10432, <https://doi.org/10.1073/pnas.0502066102>.
- [40] H. Lin, R. Bhatia, R. Lal, Amyloid  $\beta$  protein forms ion channels: implications for Alzheimer's disease pathophysiology, *FASEB J.* 15 (2001) 2433–2444, <https://doi.org/10.1096/fj.01-0377.com>.
- [41] D.C. Bode, M. Freeley, J. Nield, M. Palma, J.H. Viles, Amyloid- $\beta$  oligomers have a profound detergent-like effect on lipid membrane bilayers, imaged by atomic force and electron microscopy, *J. Biol. Chem.* 294 (2019) 7566–7572, <https://doi.org/10.1074/jbc.AC118.007195>.
- [42] M. Michikawa, J. Gong, Q. Fan, N. Sawamura, K. Yanagisawa, A novel action of Alzheimer's amyloid  $\beta$ -protein (A $\beta$ ): oligomeric A $\beta$  promotes lipid release, *J. Neurosci.* 21 (2001) 7226–7235, <https://doi.org/10.1523/JNEUROSCI.21-18-07226.2001>.
- [43] D. Mrdenovic, M. Majewska, I.S. Pieta, P. Bernatowicz, R. Nowakowski, W. Kutner, J. Lipkowski, P. Pieta, Size-dependent interaction of amyloid  $\beta$  oligomers with brain total lipid extract bilayer—fibrillation versus membrane destruction, *Langmuir* 35 (2019) 11940–11949, <https://doi.org/10.1021/acs.langmuir.9b01645>.
- [44] W. Qiang, W.-M. Yau, J. Schulte, Fibrillation of  $\beta$  amyloid peptides in the presence of phospholipid bilayers and the consequent membrane disruption, *Biochim. Biophys. Acta Biomembr.* 2015 (1848) 266–276, <https://doi.org/10.1016/j.bbmem.2014.04.011>.
- [45] D.A. Delgado, K. Doherty, Q. Cheng, H. Kim, D. Xu, H. Dong, C. Grewer, W. Qiang, Distinct membrane disruption pathways are induced by 40-residue  $\beta$ -amyloid peptides, *J. Biol. Chem.* 291 (2016) 12233–12244, <https://doi.org/10.1074/jbc.M116.720656>.
- [46] W. Qiang, R.D. Akinlolu, M. Nam, N. Shu, Structural evolution and membrane interaction of the 40-residue  $\beta$  amyloid peptides: differences in the initial proximity between peptides and the membrane bilayer studied by solid-state nuclear magnetic resonance spectroscopy, *Biochemistry* 53 (2014) 7503–7514, <https://doi.org/10.1021/bi501003n>.
- [47] M.G. Zagorski, J. Yang, H. Shao, K. Ma, H. Zeng, A. Hong, Methodological and chemical factors affecting amyloid  $\beta$  peptide amyloidogenicity, *Methods Enzymol.* (1999) 189–204, [https://doi.org/10.1016/S0076-6879\(99\)09015-1](https://doi.org/10.1016/S0076-6879(99)09015-1).
- [48] S. Linse, Mechanism of amyloid protein aggregation and the role of inhibitors, *Pure Appl. Chem.* 91 (2019) 211–229, <https://doi.org/10.1515/pac-2018-1017>.
- [49] S.-C. Jao, K. Ma, J. Talafous, R. Orlando, M.G. Zagorski, Trifluoroacetic acid pretreatment reproducibly disaggregates the amyloid  $\beta$ -peptide, *Amyloid* 4 (1997) 240–252, <https://doi.org/10.3109/13506129709003835>.
- [50] W.B. Stine, L. Jungbauer, C. Yu, M.J. LaDu, Preparing synthetic A $\beta$  in different aggregation states, in: E.D. Roberson (Ed.), *Alzheimer's Dis. Front. Dement. Methods Protoc*, Humana Press, Totowa, NJ, United States, 2010, pp. 13–32, [https://doi.org/10.1007/978-1-60761-744-0\\_2](https://doi.org/10.1007/978-1-60761-744-0_2).
- [51] Y. Fezoui, D.M. Hartley, J.D. Harper, R. Khurana, D.M. Walsh, M.M. Condron, D. J. Selkoe, P.T. Lansbury, A.L. Fink, D.B. Teplow, An improved method of preparing the amyloid  $\beta$ -protein for fibrillogenesis and neurotoxicity experiments, *Amyloid* 7 (2000) 166–178, <https://doi.org/10.3109/13506120009146831>.
- [52] R. Kodali, R. Wetzel, Polymorphism in the intermediates and products of amyloid assembly, *Curr. Opin. Struct. Biol.* 17 (2007) 48–57, <https://doi.org/10.1016/j.sbi.2007.01.007>.
- [53] S. De, D.C. Wirthensohn, P. Flagmeier, C. Hughes, F.A. Aprile, F.S. Ruggeri, D. R. Whiten, D. Emin, Z. Xia, J.A. Varela, P. Sormanni, F. Kundel, T.P.J. Knowles, C. M. Dobson, C. Bryant, M. Vendruscolo, D. Klenerman, Different soluble aggregates of A $\beta$ 42 can give rise to cellular toxicity through different mechanisms, *Nat. Commun.* 10 (2019) 1541, <https://doi.org/10.1038/s41467-019-09477-3>.
- [54] S. De, D.R. Whiten, F.S. Ruggeri, C. Hughes, M. Rodrigues, D.I. Sideris, C. G. Taylor, F.A. Aprile, S. Muyltermans, T.P.J. Knowles, M. Vendruscolo, C. Bryant, K. Blennow, I. Skoog, S. Kern, H. Zetterberg, D. Klenerman, Soluble aggregates present in cerebrospinal fluid change in size and mechanism of toxicity during Alzheimer's disease progression, *Acta Neuropathol. Commun.* 7 (2019) 120, <https://doi.org/10.1186/s40478-019-0777-4>.
- [55] B. Mannini, E. Mulvihill, C. Sgromo, R. Cascella, R. Khodarahmi, M. Ramazzotti, C.M. Dobson, C. Cecchi, F. Chiti, Toxicity of protein oligomers is rationalized by a function combining size and surface hydrophobicity, *ACS Chem. Biol.* 9 (2014) 2309–2317, <https://doi.org/10.1021/cb500505m>.
- [56] B. Bolognesi, J.R. Kumita, T.P. Barros, E.K. Esbjorn, L.M. Luheshi, D. C. Crowther, M.R. Wilson, C.M. Dobson, G. Favrin, J.J. Yerbury, ANS binding reveals common features of cytotoxic amyloid species, *ACS Chem. Biol.* 5 (2010) 735–740, <https://doi.org/10.1021/cb1001203>.
- [57] A.R.A. Ladiwala, J. Litt, R.S. Kane, D.S. Aucoin, S.O. Smith, S. Ranjan, J. Davis, W.E. Van Nostrand, P.M. Tessier, Conformational differences between two amyloid  $\beta$  oligomers of similar size and dissimilar toxicity, *J. Biol. Chem.* 287 (2012) 24765–24773, <https://doi.org/10.1074/jbc.M111.329763>.
- [58] R. Ahmed, M. Akcan, A. Khondker, M.C. Rheinstädter, J.C. Bozelli, R.M. Epan, V. Huynh, R.G. Wylie, S. Boulton, J. Huang, C.P. Verschoor, G. Melacini, Atomic resolution map of the soluble amyloid beta assembly toxic surfaces, *Chem. Sci.* 10 (2019) 6072–6082, <https://doi.org/10.1039/C9SC01331H>.
- [59] D.A. Ryan, W.C. Narrow, H.J. Federoff, W.J. Bowers, An improved method for generating consistent soluble amyloid-beta oligomer preparations for in vitro neurotoxicity studies, *J. Neurosci. Methods* 190 (2010) 171–179, <https://doi.org/10.1016/j.jneumeth.2010.05.001>.
- [60] P.T. Wong, J.A. Schauerte, K.C. Wisser, H. Ding, E.L. Lee, D.G. Steel, A. Gafni, Amyloid- $\beta$  membrane binding and permeabilization are distinct processes influenced separately by membrane charge and fluidity, *J. Mol. Biol.* 386 (2009) 81–96, <https://doi.org/10.1016/j.jmb.2008.11.060>.
- [61] T. Yasumoto, Y. Takamura, M. Tsuji, T. Watanabe-Nakayama, K. Imamura, H. Inoue, S. Nakamura, T. Inoue, A. Kimura, S. Yano, H. Nishijo, Y. Kiuchi, D. B. Teplow, K. Ono, High molecular weight amyloid  $\beta$  1–42 oligomers induce neurotoxicity via plasma membrane damage, *FASEB J.* 33 (2019) 9220–9234, <https://doi.org/10.1096/fj.20190604R>.
- [62] A. Eckert, S. Hauptmann, I. Scherping, J. Meinhardt, V. Rhein, S. Dröse, U. Brandt, M. Fändrich, W.E. Müller, J. Götz, Oligomeric and fibrillar species of  $\beta$ -amyloid (A $\beta$ 42) both impair mitochondrial function in P301L tau transgenic mice, *J. Mol. Med.* 86 (2008) 1255–1267, <https://doi.org/10.1007/s00109-008-0391-6>.
- [63] E. Cerf, R. Sarroukh, S. Tamamizu-Kato, L. Breydo, S. Derclaye, Y.F. Dufrêne, V. Narayanaswami, E. Goormaghtigh, J.-M. Ruyschaert, V. Raussens, Antiparallel  $\beta$ -sheet: a signature structure of the oligomeric amyloid  $\beta$ -peptide, *Biochem. J.* 421 (2009) 415–423, <https://doi.org/10.1042/BJ20090379>.
- [64] J.C. Stroud, C. Liu, P.K. Teng, D. Eisenberg, Toxic fibrillar oligomers of amyloid- $\beta$  have cross- $\beta$  structure, *Proc. Natl. Acad. Sci.* 109 (2012) 7717–7722, <https://doi.org/10.1073/pnas.1203193109>.
- [65] M. Vivoli Vega, R. Cascella, S.W. Chen, G. Fusco, A. De Simone, C.M. Dobson, C. Cecchi, F. Chiti, The toxicity of misfolded protein oligomers is independent of their secondary structure, *ACS Chem. Biol.* 14 (2019) 1593–1600, <https://doi.org/10.1021/acscchembio.9b00324>.
- [66] M. Ahmed, J. Davis, D. Aucoin, T. Sato, S. Ahuja, S. Aimoto, J.I. Elliott, W.E. Van Nostrand, S.O. Smith, Structural conversion of neurotoxic amyloid- $\beta$ 1–42 oligomers to fibrils, *Nat. Struct. Mol. Biol.* 17 (2010) 561–567, <https://doi.org/10.1038/nsmb.1799>.
- [67] H.A. Lashuel, D. Hartley, B.M. Petre, T. Walz, P.T. Lansbury, Amyloid pores from pathogenic mutations, *Nature* 418 (2002), <https://doi.org/10.1038/418291a>, 291–291.
- [68] R. Kaye, A. Pensalfini, L. Margol, Y. Sokolov, F. Sarsoza, E. Head, J. Hall, C. Glabe, Annular protofibrils are a structurally and functionally distinct type of

- amyloid oligomer, *J. Biol. Chem.* 284 (2009) 4230–4237, <https://doi.org/10.1074/jbc.M808591200>.
- [69] M. Serra-Batiste, M. Ninot-Pedrosa, M. Bayoumi, M. Gairí, G. Maglia, N. Carulla, A $\beta$ 42 assembles into specific  $\beta$ -barrel pore-forming oligomers in membrane-mimicking environments, *Proc. Natl. Acad. Sci.* 113 (2016) 10866–10871, <https://doi.org/10.1073/pnas.1605104113>.
- [70] H. Jang, J. Zheng, R. Nussinov, Models of  $\beta$ -amyloid ion channels in the membrane suggest that channel formation in the bilayer is a dynamic process, *Biophys. J.* 93 (2007) 1938–1949, <https://doi.org/10.1529/biophysj.107.110148>.
- [71] H. Jang, J. Zheng, R. Lal, R. Nussinov, New structures help the modeling of toxic amyloid $\beta$  ion channels, *Trends Biochem. Sci.* 33 (2008) 91–100, <https://doi.org/10.1016/j.tibs.2007.10.007>.
- [72] N. Arispe, H.B. Pollard, E. Rojas, Giant multilevel cation channels formed by alzheimer disease amyloid beta-protein [A beta P-(1–40)] in bilayer membranes, *Proc. Natl. Acad. Sci.* 90 (1993) 10573–10577, <https://doi.org/10.1073/pnas.90.22.10573>.
- [73] H. Lin, Y.J. Zhu, R. Lal, Amyloid  $\beta$  protein (1–40) forms calcium-permeable, Zn<sup>2+</sup>-Sensitive Channel in reconstituted lipid vesicles, *Biochemistry* 38 (1999) 11189–11196, <https://doi.org/10.1021/bi982997c>.
- [74] S.K. Rhee, A.P. Quist, R. Lal, Amyloid  $\beta$  protein-(1–42) forms calcium-permeable, Zn<sup>2+</sup>-sensitive channel, *J. Biol. Chem.* 273 (1998) 13379–13382, <https://doi.org/10.1074/jbc.273.22.13379>.
- [75] J. Lee, Y.H. Kim, F.T. Arce, A.L. Gillman, H. Jang, B.L. Kagan, R. Nussinov, J. Yang, R. Lal, Amyloid  $\beta$  ion channels in a membrane comprising brain total lipid extracts, *ACS Chem. Neurosci.* 8 (2017) 1348–1357, <https://doi.org/10.1021/acschemneuro.7b00006>.
- [76] D.C. Bode, M.D. Baker, J.H. Viles, Ion Channel formation by amyloid- $\beta$  42 oligomers but not amyloid- $\beta$  40 in cellular membranes, *J. Biol. Chem.* 292 (2017) 1404–1413, <https://doi.org/10.1074/jbc.M116.762526>.
- [77] A. Jan, O. Gokce, R. Luthi-Carter, H.A. Lashuel, The ratio of monomeric to aggregated forms of A $\beta$ 40 and A $\beta$ 42 is an important determinant of amyloid- $\beta$  aggregation, fibrillogenesis, and toxicity, *J. Biol. Chem.* 283 (2008) 28176–28189, <https://doi.org/10.1074/jbc.M803159200>.
- [78] I. Kuperstein, K. Broersen, I. Benilova, J. Rozenski, W. Jonckheere, M. Debulpaep, A. Vandersteen, I. Segers-Nolten, K. Van Der Werf, V. Subramanian, D. Braeken, G. Callewaert, C. Bartic, R. D'Hooge, I.C. Martins, F. Rousseau, J. Schymkowitz, B. De Strooper, Neurotoxicity of Alzheimer's disease A $\beta$  peptides is induced by small changes in the A $\beta$ 42 to A $\beta$ 40 ratio, *EMBO J.* 29 (2010) 3408–3420, <https://doi.org/10.1038/emboj.2010.211>.
- [79] G. Bitan, M.D. Kirkitadze, A. Lomakin, S.S. Vollers, G.B. Benedek, D.B. Teplow, Amyloid  $\beta$ -protein (A $\beta$ ) assembly: A $\beta$ 40 and A $\beta$ 42 oligomerize through distinct pathways, *Proc. Natl. Acad. Sci.* 100 (2003) 330–335, <https://doi.org/10.1073/pnas.222681699>.
- [80] S. Côté, R. Laghaei, P. Derreumaux, N. Mousseau, Distinct dimerization for various alloforms of the amyloid-beta protein: A $\beta$  1–40, A $\beta$  1–42, and A $\beta$  1–40 (D23N), *J. Phys. Chem. B* 116 (2012) 4043–4055, <https://doi.org/10.1021/jp2126366>.
- [81] B. Barz, B. Urbanc, Dimer formation enhances structural differences between amyloid  $\beta$ -protein (1–40) and (1–42): an explicit-solvent molecular dynamics study, *PLoS One* 7 (2012), e34345, <https://doi.org/10.1371/journal.pone.0034345>.
- [82] M. Ewald, S. Henry, E. Lambert, C. Feuillie, C. Bobo, C. Cullin, S. Lecomte, M. Molinari, High speed atomic force microscopy to investigate the interactions between toxic A $\beta$  1–42 peptides and model membranes in real time: impact of the membrane composition, *Nanoscale* 11 (2019) 7229–7238, <https://doi.org/10.1039/C8NR08714H>.
- [83] S. Henry, N.B. Bercu, C. Bobo, C. Cullin, M. Molinari, S. Lecomte, Interaction of A $\beta$  1–42 peptide or their variant with model membrane of different composition probed by infrared nanospectroscopy, *Nanoscale* 10 (2018) 936–940, <https://doi.org/10.1039/C7NR07489A>.
- [84] E. Drolle, A. Negoda, K. Hammond, E. Pavlov, Z. Leonenko, Changes in lipid membranes may trigger amyloid toxicity in Alzheimer's disease, *PLoS One* 12 (2017), e0182194, <https://doi.org/10.1371/journal.pone.0182194>.
- [85] E.J. Fernández-Pérez, F.J. Sepúlveda, R. Peoples, L.G. Aguayo, Role of membrane GM1 on early neuronal membrane actions of A $\beta$  during onset of Alzheimer's disease, *Biochim. Biophys. Acta Mol. Basis Dis.* 2017 (1863) 3105–3116, <https://doi.org/10.1016/j.bbdis.2017.08.013>.
- [86] J. Habchi, S. Chia, C. Galvagnion, T.C.T. Michaels, M.M.J. Bellaiche, F.S. Ruggeri, M. Sanguanini, I. Idini, J.R. Kumita, E. Sparr, S. Linse, C.M. Dobson, T.P. J. Knowles, M. Vendruscolo, Cholesterol catalyses A $\beta$ 42 aggregation through a heterogeneous nucleation pathway in the presence of lipid membranes, *Nat. Chem.* 10 (2018) 673–683, <https://doi.org/10.1038/s41557-018-0031-x>.
- [87] P. Scheltens, K. Blennow, M.M.B. Breteler, B. de Strooper, G.B. Frisoni, S. Salloway, W.M. Van der Flier, Alzheimer's disease, *Lancet* 388 (2016) 505–517, [https://doi.org/10.1016/S0140-6736\(15\)01124-1](https://doi.org/10.1016/S0140-6736(15)01124-1).
- [88] L. Gremer, D. Schölzel, C. Schenk, E. Reinartz, J. Labahn, R.B.G. Ravelli, M. Tusche, C. Lopez-Iglesias, W. Hoyer, H. Heise, D. Willbold, G.F. Schröder, Fibril structure of amyloid- $\beta$ (1–42) by cryo-electron microscopy, *Science* (80-) 358 (2017) 116–119, <https://doi.org/10.1126/science.aao2825>.
- [89] W. Hoyer, C. Grönwall, A. Jonsson, S. Ståhl, T. Hård, Stabilization of a  $\beta$ -hairpin in monomeric Alzheimer's amyloid- $\beta$  peptide inhibits amyloid formation, *Proc. Natl. Acad. Sci.* 105 (2008) 5099–5104, <https://doi.org/10.1073/pnas.0711731105>.
- [90] L. Gu, C. Liu, J.C. Stroud, S. Ngo, L. Jiang, Z. Guo, Antiparallel triple-strand architecture for prefibrillar A $\beta$ 42 oligomers, *J. Biol. Chem.* 289 (2014) 27300–27313, <https://doi.org/10.1074/jbc.M114.569004>.
- [91] B. Chandara, D. Bhowmik, B.K. Maity, K.R. Mote, D. Dhara, R. Venkatramani, S. Maiti, P.K. Madhu, Major reaction coordinates linking transient amyloid- $\beta$  oligomers to fibrils measured at atomic level, *Biophys. J.* 113 (2017) 805–816, <https://doi.org/10.1016/j.bpj.2017.06.068>.
- [92] G. Chen, T. Xu, Y. Yan, Y. Zhou, Y. Jiang, K. Melcher, H.E. Xu, Amyloid beta: structure, biology and structure-based therapeutic development, *Acta Pharmacol. Sin.* 38 (2017) 1205–1235, <https://doi.org/10.1038/aps.2017.28>.
- [93] C. Morris, S. Cupples, T.W. Kent, E.A. Elbassal, E.P. Wojcikiewicz, P. Yi, D. Du, N-terminal charged residues of amyloid- $\beta$  peptide modulate amyloidogenesis and interaction with lipid membrane, *Chem. Eur. J.* 24 (2018) 9494–9498, <https://doi.org/10.1002/chem.201801805>.
- [94] S.K.T.S. Wärmländer, N. Österlund, C. Wallin, J. Wu, J. Luo, A. Tiiman, J. Jarvet, A. Gråslund, Metal binding to the amyloid- $\beta$  peptides in the presence of biomembranes: potential mechanisms of cell toxicity, *JBC, J. Biol. Inorg. Chem.* 24 (2019) 1189–1196, <https://doi.org/10.1007/s00775-019-01723-9>.
- [95] D. Mrdenovic, P. Zarzycki, M. Majewska, I.S. Pieta, R. Nowakowski, W. Kutner, J. Lipkowski, P. Pieta, Inhibition of amyloid  $\beta$ -induced lipid membrane permeation and amyloid  $\beta$  aggregation by K162, *ACS Chem. Neurosci.* 12 (2021) 531–541, <https://doi.org/10.1021/acscchemneuro.0c00754>.
- [96] E.M. Sigurdsson, *Amyloid Proteins*, Humana Press, New Jersey, 2004, <https://doi.org/10.1385/1592598749>.
- [97] B.L. Nilsson, T.M. Doran, *Peptide Self-Assembly*, Springer New York, New York, NY, 2018, <https://doi.org/10.1007/978-1-4939-7811-3>.
- [98] B. Ma, R. Nussinov, Polymorphic C-terminal  $\beta$ -sheet interactions determine the formation of fibril or amyloid  $\beta$ -derived diffusible ligand-like globulomer for the alzheimer A $\beta$ 42 dodecamer, *J. Biol. Chem.* 285 (2010) 37102–37110, <https://doi.org/10.1074/jbc.M110.133488>.
- [99] S. Barghorn, V. Nimmrich, A. Striebing, C. Krantz, P. Keller, B. Janson, M. Bahr, M. Schmidt, R.S. Bitner, J. Harlan, E. Barlow, U. Ebert, H. Hillen, Globular amyloid beta-peptide1-42 oligomer - a homogenous and stable neuropathological protein in Alzheimer's disease, *J. Neurochem.* 95 (2005) 834–847, <https://doi.org/10.1111/j.1471-4159.2005.03407.x>.
- [100] Z. Fu, D. Aucoin, J. Davis, W.E. Van Nostrand, S.O. Smith, Mechanism of nucleated conformational conversion of A $\beta$ 42, *Biochemistry* 54 (2015) 4197–4207, <https://doi.org/10.1021/acs.biochem.5b00467>.
- [101] L.J. Pike, Lipid rafts: bringing order to chaos, *J. Lipid Res.* 44 (2003) 655–667, <https://doi.org/10.1194/jlr.R200021-JLR200>.
- [102] C.-L. Schengrund, Lipid rafts: keys to neurodegeneration, *Brain Res. Bull.* 82 (2010) 7–17, <https://doi.org/10.1016/j.brainresbull.2010.02.013>.
- [103] S. Henry, H. Vignaud, C. Bobo, M. Decossas, O. Lambert, E. Harte, I.D. Alves, C. Cullin, S. Lecomte, Interaction of A $\beta$  1–42 amyloids with lipids promotes "Off-Pathway" oligomerization and membrane damage, *Biomacromolecules* 16 (2015) 944–950, <https://doi.org/10.1021/bm501837w>.
- [104] E.Y. Chi, C. Ege, A. Winans, J. Majewski, G. Wu, K. Kjaer, K.Y.C. Lee, Lipid membrane templates the ordering and induces the fibrillogenesis of Alzheimer's disease amyloid- $\beta$  peptide, *Proteins: Struct., Funct., Bioinf.* 72 (2008) 1–24, <https://doi.org/10.1002/prot.21887>.
- [105] K. Ikeda, K. Matsuzaki, Driving force of binding of amyloid  $\beta$ -protein to lipid bilayers, *Biochem. Biophys. Res. Commun.* 370 (2008) 525–529, <https://doi.org/10.1016/j.bbrc.2008.03.130>.
- [106] C. Ege, K.Y.C. Lee, Insertion of Alzheimer's A $\beta$ 40 peptide into lipid monolayers, *Biophys. J.* 87 (2004) 1732–1740, <https://doi.org/10.1529/biophysj.104.043265>.
- [107] M. Bokvist, F. Lindström, A. Watts, G. Gröbner, Two types of Alzheimer's  $\beta$ -amyloid (1–40) peptide membrane interactions: aggregation preventing transmembrane anchoring versus accelerated surface fibril formation, *J. Mol. Biol.* 335 (2004) 1039–1049, <https://doi.org/10.1016/j.jmb.2003.11.046>.
- [108] M.F.M. Sciacca, S.A. Kotler, J.R. Brender, J. Chen, D. Lee, A. Ramamoorthy, Two-step mechanism of membrane disruption by A $\beta$  through membrane fragmentation and pore formation, *Biophys. J.* 103 (2012) 702–710, <https://doi.org/10.1016/j.bpj.2012.06.045>.
- [109] M.R.R. de Planque, V. Raussens, S.A. Contera, D.T.S. Rijkers, R.M.J. Liskamp, J.-M. Ruyschaert, J.F. Ryan, F. Separovic, A. Watts,  $\beta$ -sheet structured  $\beta$ -Amyloid (1–40) perturbs phosphatidylcholine model membranes, *J. Mol. Biol.* 368 (2007) 982–997, <https://doi.org/10.1016/j.jmb.2007.02.063>.
- [110] E.E. Ambroggio, D.H. Kim, F. Separovic, C.J. Barrow, K.J. Barnham, L. A. Bagatolli, G.D. Fidelio, Surface behavior and lipid interaction of alzheimer  $\beta$ -amyloid peptide 1–42: a membrane-disrupting peptide, *Biophys. J.* 88 (2005) 2706–2713, <https://doi.org/10.1529/biophysj.104.055582>.
- [111] K.J. Korshavn, C. Satriano, Y. Lin, R. Zhang, M. Dulchavsky, A. Bhunia, M. I. Ivanova, Y.-H. Lee, C. La Rosa, M.H. Lim, A. Ramamoorthy, Reduced lipid bilayer thickness regulates the aggregation and cytotoxicity of amyloid- $\beta$ , *J. Biol. Chem.* 292 (2017) 4638–4650, <https://doi.org/10.1074/jbc.M116.764092>.
- [112] Y. Nakazawa, Y. Suzuki, M.P. Williamson, H. Saito, T. Asakura, The interaction of amyloid A $\beta$ (1–40) with lipid bilayers and ganglioside as studied by 31P solid-state NMR, *Chem. Phys. Lipids* 158 (2009) 54–60, <https://doi.org/10.1016/j.chemphyslip.2008.12.001>.
- [113] E.Y. Chi, S.L. Frey, K.Y.C. Lee, Ganglioside GM1-mediated amyloid-beta fibrillogenesis and membrane disruption, *Biochemistry* 46 (2007) 1913–1924, <https://doi.org/10.1021/bi062177x>.
- [114] Q. Cheng, Z.-W. Hu, K.E. Doherty, Y.J. Tobin-Miyaji, W. Qiang, The on-fibrillation-pathway membrane content leakage and off-fibrillation-pathway lipid mixing induced by 40-residue  $\beta$ -amyloid peptides in biologically relevant model



- liposomes, *Biochim. Biophys. Acta Biomembr.* 2018 (1860) 1670–1680, <https://doi.org/10.1016/j.bbamem.2018.03.008>.
- [115] R.D. Akinlolu, M. Nam, W. Qiang, Competition between fibrillation and induction of vesicle fusion for the membrane-associated 40-residue  $\beta$ -amyloid peptides, *Biochemistry* 54 (2015) 3416–3419, <https://doi.org/10.1021/acs.biochem.5b00321>.
- [116] C. La Rosa, S. Scalisi, F. Lolicato, M. Pannuzzo, A. Raudino, Lipid-assisted protein transport: a diffusion-reaction model supported by kinetic experiments and molecular dynamics simulations, *J. Chem. Phys.* 144 (2016), 184901, <https://doi.org/10.1063/1.4948323>.
- [117] M.F. Sciacca, F. Lolicato, C. Tempa, F. Scollo, B.R. Sahoo, M.D. Watson, S. García-Viñuales, D. Milardi, A. Raudino, J.C. Lee, A. Ramamoorthy, C. La Rosa, Lipid-chaperone hypothesis: a common molecular mechanism of membrane disruption by intrinsically disordered proteins, *ACS Chem. Neurosci.* 11 (2020) 4336–4350, <https://doi.org/10.1021/acscemneuro.0c00588>.
- [118] H. Fatafta, B. Kav, B.F. Bundschuh, J. Loschwitz, B. Strodel, Disorder-to-order transition of the amyloid- $\beta$  peptide upon lipid binding, *Biophys. Chem.* 280 (2022), 106700, <https://doi.org/10.1016/j.bpc.2021.106700>.
- [119] F. Scollo, C. Tempa, F. Lolicato, M.F.M. Sciacca, A. Raudino, D. Milardi, C. La Rosa, Phospholipids critical micellar concentrations trigger different mechanisms of intrinsically disordered proteins interaction with model membranes, *J. Phys. Chem. Lett.* 9 (2018) 5125–5129, <https://doi.org/10.1021/acs.jpcclett.8b02241>.
- [120] F. Scollo, C. La Rosa, Amyloidogenic intrinsically disordered proteins: new insights into their self-assembly and their interaction with membranes, *Life* 10 (2020) 1–20, <https://doi.org/10.3390/life10080144>.
- [121] C. La Rosa, M. Condorelli, G. Compagnini, F. Lolicato, D. Milardi, T.N. Do, M. Karttunen, M. Pannuzzo, A. Ramamoorthy, F. Fraternali, F. Collu, H. Rezaei, B. Strodel, A. Raudino, Symmetry-breaking transitions in the early steps of protein self-assembly, *Eur. Biophys. J.* 49 (2020) 175–191, <https://doi.org/10.1007/s00249-020-01424-1>.